




Article

Assessing Data Fusion in Sensory Devices for Enhanced Prostate Cancer Detection Accuracy

Jeniffer Katherine Carrillo Gómez ^{1,2,*} , Carlos Alberto Cuastumal Vásquez ¹ , Cristhian Manuel Durán Acevedo ^{1,*} 
and Jesús Brezmes Llecha ²

¹ GISM Group, Department of EEST, University of Pamplona, Pamplona 543050, Colombia; carlos.cuastumal@unipamplona.edu.co

² MIL@B Group, Department of Electronic Engineering, University Rovira i Virgili, 43007 Tarragona, Spain; jesus.brezmes@urv.cat

* Correspondence: jeniffer.carrillo@unipamplona.edu.co (J.K.C.G.); cmduran@unipamplona.edu.co (C.M.D.A.); Tel.: +57-312-4092247 (J.K.C.G.); +57-311-2135846 (C.M.D.A.)

Abstract: The combination of an electronic nose and an electronic tongue represents a significant advance in the pursuit of effective detection methods for prostate cancer, a widespread form of cancer affecting men across the globe. These cutting-edge devices, collectively called “E-Senses”, use data fusion to identify distinct chemical compounds in exhaled breath and urine samples, potentially improving existing diagnostic techniques. This study combined the information from two sensory perception devices to detect prostate cancer in biological samples (breath and urine). To achieve this, data from patients diagnosed with the disease and from control individuals were collected using a gas sensor array and chemical electrodes. The signals were subjected to data preprocessing algorithms to prepare them for analysis. Following this, the datasets for each device were individually analyzed and subsequently merged to enhance the classification results. The data fusion was assessed and it successfully improved the accuracy of detecting prostate-related conditions and distinguishing healthy patients, achieving the highest success rate possible (100%) in classification through machine learning methods, outperforming the results obtained from individual electronic devices.

Keywords: prostate cancer; data fusion; eNose; eTongue; machine learning



Citation: Gómez, J.K.C.; Vásquez, C.A.C.; Acevedo, C.M.D.; Llecha, J.B. Assessing Data Fusion in Sensory Devices for Enhanced Prostate Cancer Detection Accuracy. *Chemosensors* **2024**, *12*, 228. <https://doi.org/10.3390/chemosensors12110228>

Received: 26 September 2024

Revised: 23 October 2024

Accepted: 30 October 2024

Published: 1 November 2024



Copyright: © 2024 by the authors. Licensee MDPI, Basel, Switzerland. This article is an open access article distributed under the terms and conditions of the Creative Commons Attribution (CC BY) license (<https://creativecommons.org/licenses/by/4.0/>).

1. Introduction

Prostate cancer (PCa) is one of the most prevalent malignant neoplasms in men worldwide, with a high incidence rate that makes it the second most diagnosed type of cancer in the male population. According to a Global Cancer Observatory (GCO) report, PCa represents a major public health concern, ranking fifth as a cause of death from cancer among men [1]. Studies on PCa have reported that incidence and mortality rates can be influenced by external factors [2–4]. Countries with greater social and economic development generally tend to have a higher incidence of PCa. This is mainly due to better access to medical services, including preventive health check-ups and PCa screening programs, which vary from country to country [5,6].

In its early stages, PCa often presents with no symptoms, making it difficult to detect without specific tests; however, symptoms, such as urinary problems, pelvic pain, or blood in urine, may appear in more advanced stages. It is crucial to note that these symptoms may also be associated with other benign prostate conditions, such as benign prostatic hyperplasia (BPH) or prostatitis, underscoring the importance of regular medical examinations for an accurate diagnosis. An early diagnosis and proper monitoring are essential for effectively managing any prostate issue and preventing complications; the sooner the diagnosis, the better prognosis a patient will have.

Currently, the main tests for detecting PCa are the prostate-specific antigen (PSA), digital rectal examination (DRE), and transrectal biopsy, which are the optimal standards

for confirming the disease. However, the latter is a highly invasive technique, causes discomfort for patients, and may be associated with various complications, such as bleeding, temporary urinary symptoms, and others. Regarding the PSA and DRE, in recent years, there has been controversy regarding the effectiveness and accuracy of early PCa diagnosis using these methods, due to their inability by themselves to distinguish between BPH, prostatitis, and localized tumors, leading to unnecessary prostate biopsies due to false positives, and the overdiagnosis and overtreatment of PCa [7,8]. Consequently, there is a need to develop new techniques, preferably non-invasive, for the early detection of PCa to reduce the number of unnecessary prostate biopsies and procedures that affect quality of life.

Advances in artificial intelligence (AI), machine learning, and intelligent sensory technologies (E-Senses), have allowed for the proposal of innovative approaches for the early detection and characterization of various types of cancer [9–11]. These emerging technologies served as support tools, and have redefined the oncology landscape by significantly improving the precision of identifying and monitoring neoplasms at their earliest stages. E-Senses, being non-invasive tests, stand out for their speed, portability, and low cost, making them ideal solutions for implementation in rural or hard-to-reach areas, where specialized healthcare services are limited or nonexistent.

The main objective of E-Senses systems is to detect and analyze sensory characteristics through different types of sensors, pattern recognition techniques, and multivariate data analysis. Some studies reported on in the literature have proposed using electronic noses as a promising tool for the non-invasive diagnosis of PCa by analyzing biological fluids, such as urine's headspace [10,12–18] and breath [11,19,20]. These sensory devices have shown potential for identifying chemical patterns that can be used to differentiate between samples from healthy individuals and those with PCa. Similarly, using an eTongue for PCa detection is a topic that has barely been studied; however, some studies have explored its application to analyzing urine samples [9,21,22]. Overall, all the studies mentioned above, for both systems, have achieved high levels of sensitivity and specificity, individually exceeding an 80% success rate in many cases. In a previous study by Durán et al., the effectiveness of eNose and eTongue systems in detecting PCa and related diseases was evaluated using non-invasive samples of exhaled breath and urine. In that report, the eTongue system achieved an accuracy of 92.9% in classifying the samples from the PCa and the control groups, while the eNose system also achieved a high accuracy in classification, including for additional control subcategories, such as patients with BPH, prostatitis, and healthy individuals [23].

Nowadays, combining data acquired through these sensory systems can provide more precise and complete information about a sample compared to the same detection devices working individually. This improves sensory analysis's sensitivity, discrimination, and reliability, leading to more accurate diagnoses and a remarkable ability to detect and differentiate between pathological conditions [24,25]. Therefore, in previous research, there was a simple approach where the data from breath samples and urine headspace were combined using an eNose for PCa detection, achieving 95.6% accuracy, 84.55% sensitivity, 98.6% specificity, and 86.25% precision in the classification of patients with BPH, prostatitis and healthy individuals as the controls [23]. Regarding the above, the present study aims to evaluate the data fusion method, with all possible combinations, to determine if it is capable of improving the results obtained by the two devices, which have been used independently in recent reports. Therefore, for testing purposes, the odor patterns and taste profiles of the urine samples analyzed by the different sensory technologies (eNose and eTongue) were extracted, and their ability to classify patients as those with PCa or as controls was evaluated using various artificial intelligence algorithms, achieving an accuracy rate of up to 100%, based on the combination of the urine measurements acquired through the C110 and 250BT electrodes for the eTongue, the urine sample measurements obtained with the eTongue and eNose, and the measurements of urine and breath samples with both systems.

This work is the first to explore using multiple data combinations from both eNose and eTongue devices to detect prostate cancer and related conditions, such as BPH and prostatitis. This innovative method enhances the classification accuracy and demonstrates the effectiveness of using combined sensory data to improve the diagnostic capability for PCa and related diseases, setting a new benchmark for non-invasive prostate cancer diagnostics.

2. Materials and Methods

This section outlines the modules employed for the experimental tests with the ‘‘E-Senses’’ devices. Figure 1 depicts the process for detecting PCa through the following stages: (1) conditioning of the urine samples and breath, (2) data acquisition, and (3) data treatment and processing.

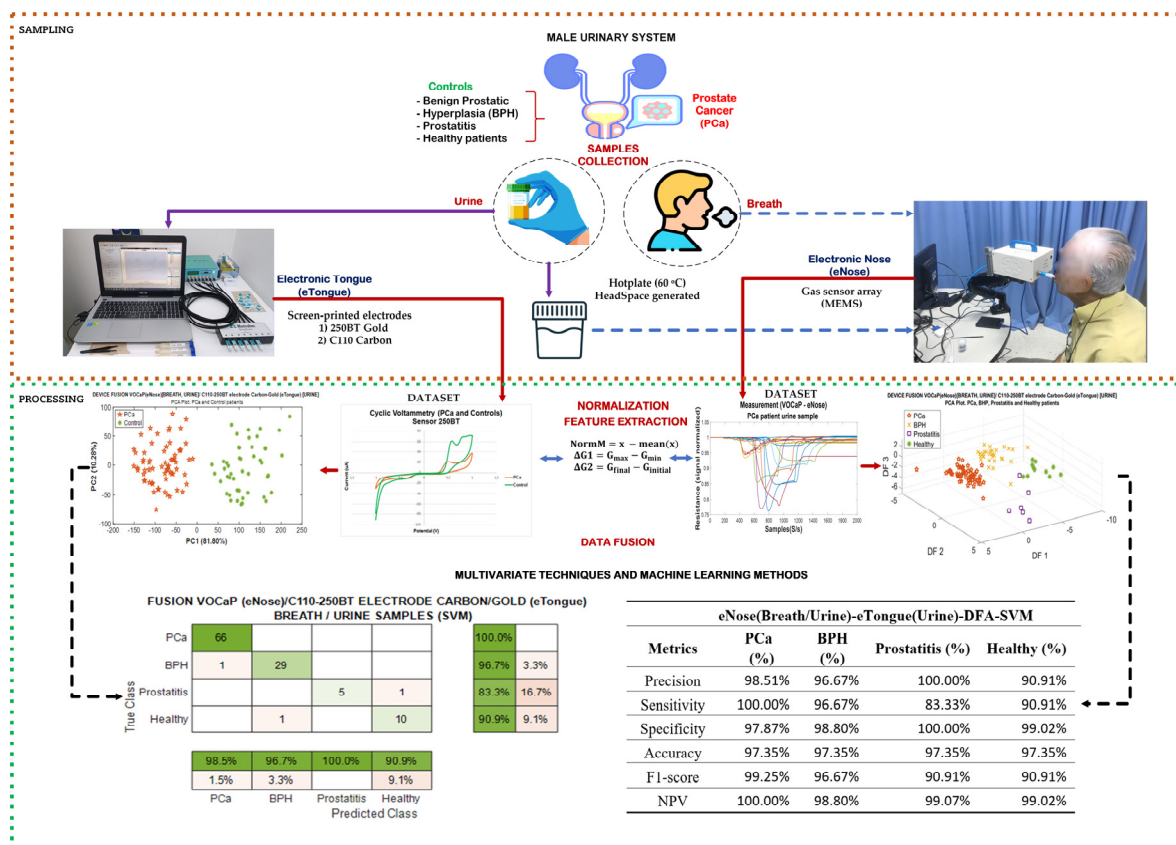


Figure 1. Scheme of E-Senses for improving PCa detection.

As shown in the figure, this study primarily focused on detecting PCa through urine samples collected for analysis using an electronic tongue. Similarly, an eNose was used to analyze the breath and urine headspace, where a set of measurements was acquired that revealed significant chemical and biological differences between patients with various prostate conditions. A μ Stat8000 potentiostat manufactured by Metrohm DropSens Company (Llanera, Spain) [26] was used for the eTongue measurements of the urine samples. Two types of screen-printed electrodes were tested in this study: carbon-based C110 and gold-based 250BT. These electrodes consist of a working electrode, an auxiliary electrode, and a reference electrode. For the operation of the eTongue, both electrodes were used in the different tests by connecting them to the potentiostat, which recorded the currents generated during the electrochemical reactions. For each acquired measurement, voltammograms were extracted to create a representative database of the samples, showing marked differences in the responses of the urine samples between those from the patients with prostate cancer and those from the controls. These differences allowed for the identification of the specific patterns associated with various prostate conditions. The purpose of testing

these two sensor types was to evaluate which one yielded better results for differentiating between and classifying the PCa patients and controls.

The exhaled breath samples were collected from volunteer patients using an eNose to detect the volatile organic compounds (VOCs) associated with the PCa and control groups. Additionally, the urine samples were heated to a temperature of 60 °C using a hotplate device to generate the headspace, obtaining gaseous samples, which were then directed into the gas sensor chamber. The signals produced by the commercial sensors, manufactured with Micro-Electro-Mechanical System (MEMS) technology, were acquired as resistance values (Ω), representing the chemical reactions, and were converted into electrical values corresponding to the VOCs present in the breath and urine (see Table 1). Therefore, as with the eTongue, the differences in these patterns allowed for the discrimination between patients with PCa and other groups.

Table 1. MEMS-type gas sensors.

Type	Sensors	No.	Manufactured	Sensitive Layers Number	Detected Compounds	Detection Limit
Digital	BME 680	2	BOSCH (Reutligen, Germany)	1	Ethanol Isoprene/2-methyl-1,3 butadiene Ethanol	5 ppm 10 ppm 10 ppm
	CCS811	2	Sciosense (Eindhoven, The Netherland)	1	eTVOC eCO ₂	0 ppm to 32,768 ppm 400 ppm to 29,206 ppm
	SPG30	2	Sensirion (Chicago, IL, USA)	2	Ethanol H ₂ TVOC CO ₂ eq	0.3 ppm to 10 ppm 0.5 ppm to 3 ppm 0 ppb to 60,000 ppb 400 ppm to 60,000 ppm
Analog	MICS 6814	1	SGX Sensortech (Neuchatel, Switzerland)	2	Carbon monoxide Nitrogen dioxide Ethanol Hydrogen Ammoniac Methane Propane Iso-butane	1 ppm to 1000 ppm 0.05 ppm to 10 ppm 10 ppm to 500 ppm 1 ppm to 1000 ppm 1 ppm to 500 ppm >1000 ppm >1000 ppm >1000 ppm
	MICS 4514	1	SGX Sensortech	3	Carbon monoxide Nitrogen dioxide Ethanol Hydrogen Ammoniac Methane	0 ppm to 1000 ppm 0.05 ppm to 10 ppm 10 ppm to 500 ppm 1 ppm to 1000 ppm 1 ppm to 500 ppm >1000 ppm
	CCS801	1	Sciosense	1	Carbon monoxide Ethanol Formaldehyde	0.1 ppm to 400 ppm 0.1 ppm to 208 ppm 0.1 ppm to 2 ppm
	GM 502B	1	Winsen Electronics (Zhengzhou, china)	1	Alcohol	1 ppm to 100 ppm
						Acetone Toluene Formaldehyde

Once the measurements were acquired, they were preprocessed through feature extraction techniques to capture the most relevant information from the dataset, including the parameters, such as signal intensity or amplitude and other factors, for sample classification. Additionally, the measurements were normalized to eliminate noise and variability, followed by multivariate analysis techniques, such as principal component analysis (PCA) and discriminant function analysis (DFA), to reduce the data dimensionality to discriminate and classify the measurements. After data preprocessing, the data fusion technique was applied to the responses generated by the two systems. Therefore, the information obtained from the two biological sources (urine and breath) was combined, creating a

more robust dataset with more significant information and improved predictive capability. Moreover, the eTongue and eNose data were processed using machine learning methods, creating training models based on algorithms, like Support Vector Machines (SVMs), Naïve Bayes, and K-Nearest Neighbors (KNN). Finally, confusion matrices, represented by the diagonals of the predictions and error rates, were used to evaluate the classification models. Here, metrics were determined with which to assess the model's performance, providing a better perspective on evaluating the model's effectiveness in classifying PCa and related conditions.

Sample Collection Process

This study's population comprised two groups: 66 patients with histopathologically confirmed PCa via biopsies, and 47 volunteers who served as the control group. Among the control group, 30 had BPH; 6 had prostatitis; and 11 were healthy individuals with no family history of PCa, no evidence of neoplastic disease, and a PSA level below 1 ng/mL. The selected patients visited the Urology Center "Uronorte S.A.", located in Cúcuta (Colombia), and both groups were aged between 50 and 89 years. In addition, each patient signed an informed consent form, where they were informed about this study's procedure, risks, and benefits. Each patient was instructed to refrain from eating and to limit fluid intake for 10 h before the urine sample collection to prevent the dilution of the sample. Additionally, the patients were asked to provide their first-morning urine, ensuring the sample was more concentrated and representative. Fifty milliliters of urine were collected from each patient in sterile containers and stored in Falcon tubes at $-20\text{ }^{\circ}\text{C}$ until analysis. As for the breath samples, they were taken directly at the Uronorte facilities.

The breath samples were collected directly using an eNose (Figure 2a) with a disposable mouthpiece equipped with a unidirectional valve to prevent backflow. The patients were instructed to exhale continuously until they could no longer do so. The eNose device collected the exhaled breath in an internal concentration chamber heated to $60\text{ }^{\circ}\text{C}$. During the process, the first portion of the exhalation (the initial 10 s) was discarded, and the device captured the last portion, known as the alveolar breath, over the next 50 s. This air sample was then sent directly into the sensor chamber for measurement. Afterward, the device switched to an ambient air for 60 s to allow the sensors to recover and return to the baseline.



Figure 2. eNose System: (a) Sampling device for breath collection using a disposable mouthpiece, (b) Sampling protocol for urine collection generating a headspace.

The urine sample collection with the eNose involved creating a headspace by heating 20 mL of centrifuged urine in a sealed container at $60\text{ }^{\circ}\text{C}$ for 30 min (see Figure 2b).

The resulting VOCs were directed into a sampling chamber maintained at $40\text{ }^{\circ}\text{C}$ to minimize humidity and prevent condensation. A constant airflow of 0.9 L/min carried the VOCs to the sensor chamber, which was kept between $39\text{ }^{\circ}\text{C}$ and $41\text{ }^{\circ}\text{C}$ with 30% relative humidity. The process started with a 2 min ambient air baseline, followed by 3 min of VOCs detection. Afterward, ambient air was flushed through the system to clean the

sensors and avoid memory effects. This protocol ensured precise VOCs measurements under controlled conditions.

For the eNose, the process started by normalizing the raw data using the “mean-centering” technique, which involved adjusting the data so that the mean value of each variable became zero. This step was conducted after calculating the steady-state parameter, defined as the difference between the maximum and minimum voltage values ($\Delta V_1 = V_{\text{Max}} - V_{\text{Min}}$), where V_{Max} = maximum voltage value and V_{Min} = minimum voltage value of the sensor responses. Once the eNose data were normalized, the orthogonal signal correction (OSC) algorithm was applied to the gas sensor signals to eliminate any systematic variations unrelated to the primary data of interest, specifically addressing signal drift [27].

For the eTongue, the same steady-state parameter (ΔV_1) was applied to the dataset through the $\Delta I_1 = I_{\text{Max}} - I_{\text{Min}}$ parameter, with the additional enhancement of calculating the initial and final current values ($\Delta I_2 = I_{\text{Final}} - I_{\text{Initial}}$) to obtain further information, where I_{Final} = final current value and I_{Initial} = initial current value of the electrode response. This technique aimed to extract more features and provide a richer data set for further analysis.

As with the eNose, the normalization method was applied to the eTongue data to standardize the measurements. Since the electrode signals showed no significant drift, using the orthogonal signal correction (OSC) algorithm was considered unnecessary to ensure the stability of the data. After completing the data preparation for both devices, principal component analysis (PCA) and discriminant function analysis (DFA) methods were applied to reduce the dimensionality of the datasets and highlight the most relevant patterns for further analysis. These methods effectively highlighted the most pertinent patterns, making it easier to uncover the underlying trends within the data. As a result, two matrices (“scores”) were generated from these multivariate analyses, with dimensions of 113×2 , from which the most significant principal components (PCs) and factors were extracted. Finally, the datasets were merged, resulting in a combined matrix providing a more comprehensive dataset for further interpretation and analysis.

It should be noted that the k-fold cross-validation method was employed to evaluate the performance of each classification model for predicting unseen data. To achieve this, the dataset was divided into smaller subsets (five folds), where the model was trained on some subsets and tested on the remaining ones. This process was repeated multiple times, using a different subset as the test set. For example, the DFA method was applied to the training data within each fold (during each split), and the test data were transformed using the DFA model trained on the training set. This method ensured consistency within the transformation application and helped avoid overfitting. The transformed test data were then evaluated using the SVM classifier, allowing for the model to be assessed on previously unseen data.

Subsequently, several performance metrics were calculated from the confusion matrices to assess the classification model’s effectiveness at detecting PCa and distinguishing it from the control cases.

3. Results

The results were divided into two phases: The first phase involved selecting the best previously published results, which showed that the best discrimination results for the two categories were achieved using PCA, and for the four categories, the best performance was obtained with the DFA classifier. Various classification models were also evaluated, and the best ones were selected to calculate the metrics. In the second phase, the most notable findings from the data fusion were determined using the previously mentioned data processing methods.

As mentioned, each analysis was based on the 113 measurements acquired from the E-Senses devices. The categories for prostate cancer and the control patients were classified, and an additional effort was made to classify the categories proposed for the control group.

3.1. eNose Data Analysis

Figure 3 shows two radar plots created to visualize four raw signals acquired with the eNose to detect the VOCs in the breath (a) and the urine samples' headspace (b). This plot is related to prostate gland conditions, such as PCa, BPH, prostatitis, and healthy states, and provides an overall description of the contribution of the variables.

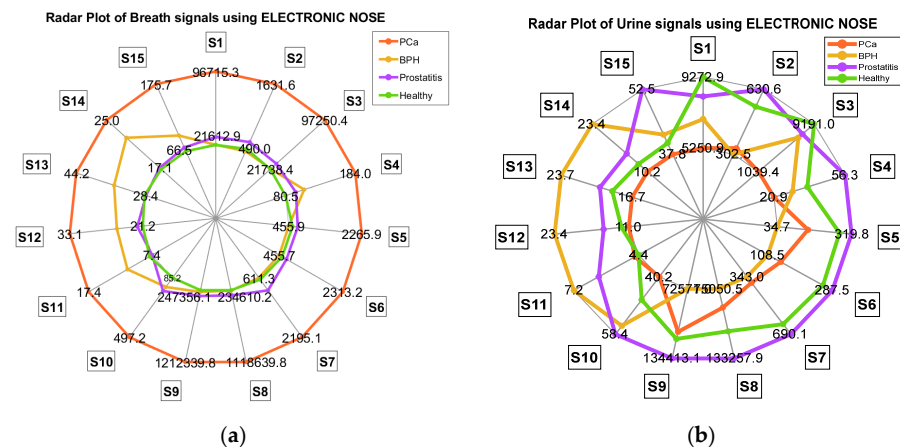


Figure 3. Radar plot of sensor responses of eNose for prostate conditions (PCa, BPH, prostatitis, and healthy patients). (a) Breath samples signals, and (b) urine samples HS signals.

The sensors (S1–S15) in the eNose system represent a different detection channel for the specific VOCs found in the breath (left) and urine (right) samples. The orange line (PCa) generally shows higher sensor responses to the breath samples, indicating higher VOCs signals. However, in the urine samples, the intensity of the PCa signals is notably lower, representing a weaker response than in the breath samples. The numerical values represent the intensity of the sensor responses, in arbitrary units corresponding to the concentration of VOCs detected.

Almost all the sensors had a significantly elevated response when sensing exhaled breath, with especially high readings for the S1, S3, S5, S6, S7, S8, and S9 gas sensors, where the signal's intensity indicates a strong response to specific gas molecules present in the breath of patients with PCa. Likewise, the urine samples show distinct peaks for sensors S1, S7, S8, and S9, with a significant difference from the breath samples. The green line represents healthy individuals and is mainly contained within the other lines, and especially shows lower responses for the breath compared to the urine samples, as there are significant variations in most of the sensors, such as S1, S3, S7, and S8, during breath detection. On the other hand, the healthy individual's profile based on the urine samples is still within the lower range compared to the disease states, but with a noticeable peak for sensors S1, S3, S7, and S8.

Nevertheless, the figures show some overlaps between BPH (yellow line), prostatitis (purple line), and healthy profiles in the breath and urine samples, demonstrating the diverse behavior of the eNose for both types of samples.

Based on the sensor data, the radar plot demonstrates that the eNose can differentiate between prostate-related conditions, such as PCa, and the control group. The important variations between the two plots underscore the importance of the sample type for detecting these conditions. Thus, it provides a preliminary visual assessment of the eNose data, which is crucial for guiding the development of data preprocessing and processing strategies, particularly in machine learning for classification tasks.

3.1.1. Urine Analysis with eNose: PCa vs. Control and PCa vs. Prostatitis, BPH, and Healthy

Figure 4a presents the PCA plot that discriminates between the PCa patients and the controls. PC1 captures almost all the information needed to differentiate between

the two groups, achieving a total data variance of 98.97%, while PC2 accounts for only 0.42%. Nevertheless, some overlap between the two groups can be observed, indicating that, although the model achieves good overall discrimination, some samples were too complex to classify correctly based on just two components.

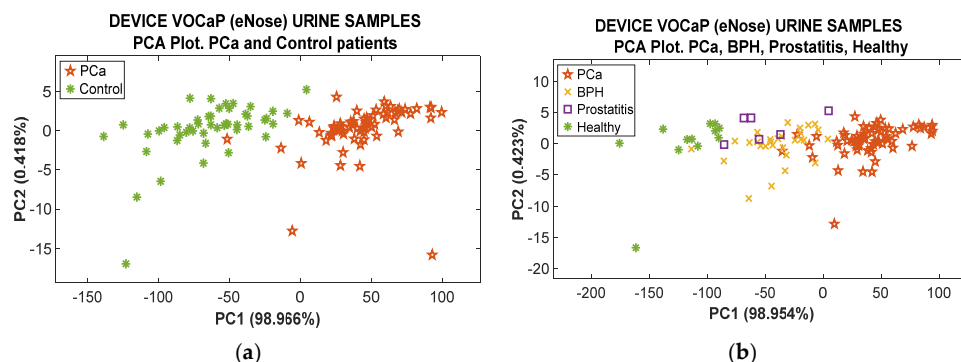


Figure 4. (a) PCA plot of PCa and control categories of urine samples using eNose, (b) PCA plot of urine samples (PCa vs. BPH, prostatitis, and healthy) using eNose.

A cross-validation method with k -fold = 5 and an SVM classifier was applied, achieving 100% success in classification. Figure 4b presents the PCA plot based on the urine samples from patients with different prostate conditions, such as PCa, BPH, and prostatitis, and those from the healthy patients, illustrating that 99% of the data variation can be captured through the first two PCs. The figure clearly distinguishes between the groups, particularly between the healthy individuals and those with PCa. Moreover, the healthy patients are primarily clustered around negative PC1 values, whereas the PCa patients have positive values, indicating significant differences in their chemical profiles.

However, there is considerable overlap between the control group's subcategories. This may be because some chemical characteristics of the urine samples are common among these categories, making precise discrimination challenging. Furthermore, the metrics presented in Table 2 show that the model based on the combination of PCA-SVM is effective at correctly classifying the urine samples of the PCa patients and controls, with the metrics reaching 100%, which were obtained using SVM to classify the PCa vs. control categories with the eNose.

Table 2. Metrics for PCA-SVM model for classifying PCa and control urine samples using eNose.

Urine-eNose-PCA-SVM		
Metrics	PCa (%)	Control (%)
Precision	100	100
Sensitivity	100	100
Specificity	100	100
Accuracy	100	100
NPV	100	100

The SVM model effectively maximizes the margin of separation using data from three dimensions (PC1, PC2, and PC3) derived from the PCA. Although some overlap may be visible in the 2D representation (PC1 and PC2), the SVM can optimize the margin of separation based on the three-dimensional data (PC1, PC2, and PC3).

Figure 5 shows the 3D DFA plot using the eNose device applied to the urine samples from the patients. The plot illustrates the classification of four distinct patient groups: PCa, BPH, prostatitis, and healthy individuals. The three axes represent the discriminant functions, which are the combinations of features used to classify the samples.

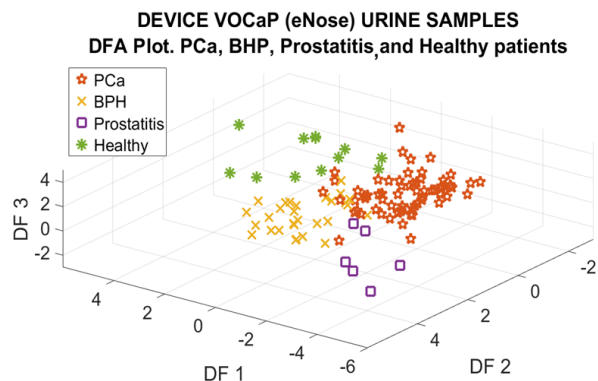


Figure 5. DFA plot for PCa and control categories classification of urine samples using eNose.

In a short analysis, PCa forms a relatively distinct cluster towards the right side of the plot, showing clear separation from the other groups along DF1 and DF2. The BPH patients occupy a different plot area, showing some similarities with the PCa group but generally remaining distinct. The prostatitis patients are more scattered, occupying a central location in the plot and being somewhat distinguishable from the other groups. The healthy patients form a clear and separate cluster, located towards the left and upper part of the plot, showing a strong separation from the diseased groups. The DFA plot successfully highlights how the eNose device can distinguish between these patient groups based on urine samples, with relatively strong separation, particularly between the healthy group and those with prostate-related conditions.

Table 3 illustrates the performance metrics obtained using a DFA–Random Forest model with a k-fold cross-validation ($k = 5$) to classify the urine samples into four categories. The metrics for this model are highly accurate, demonstrating that the eNose has an excellent capacity to identify prostate conditions along with healthy individuals. Additionally, it shows an overall accuracy of 91.2% across all the categories. However, the lower sensitivity for BPH and prostatitis indicates that these conditions may be more difficult to distinguish, possibly due to similarities in the VOCs detected by the system, making it challenging to identify these two categories.

Table 3. Metrics for DFA–Random Forest model for classifying PCa vs. BPH, prostatitis, and healthy urine samples using eNose.

Urine–eNose–DFA–Random Forest				
Metrics	PCa (%)	BPH (%)	Prostatitis (%)	Healthy (%)
Precision	90.0	92.3	100	91.6
Sensitivity	95.5	82.8	83.3	91.7
Specificity	85.1	97.6	100	99.0
Accuracy	91.2	91.2	91.2	91.2
NPV	93.0	94.3	99.1	99.0

3.1.2. Breath Analysis with eNose: PCa vs. Control and PCa vs. Prostatitis, BPH, and Healthy

In Figure 6a, it can be observed that 79.8% of the total variability in the data acquired using the eNose and breath samples from the PCa patients versus the controls is captured by PC1 and PC2. This means that nearly 80% of the information in the original samples can be captured and visualized with this plot. Regarding separating the two categories, the PCa samples are primarily located in the negative region of PC1; in contrast, the control samples are mainly located in the positive area of the same axis, indicating a difference between the patterns in each group. Only a small proportion of the PCa and control samples are classified incorrectly.

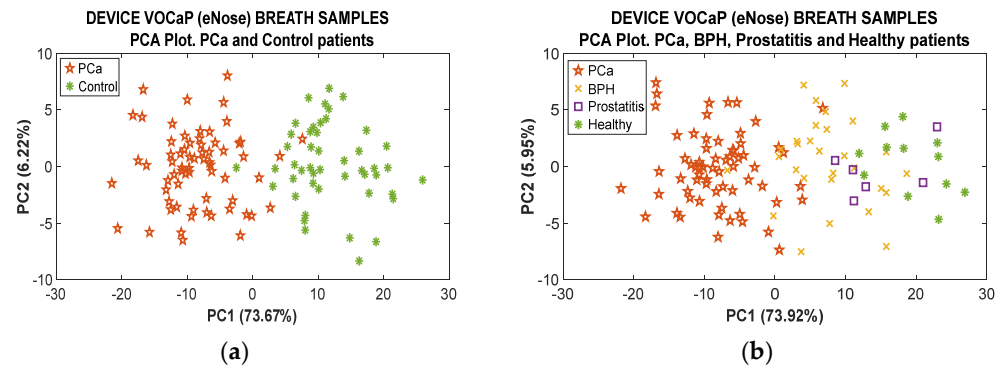


Figure 6. (a) PCA plot of PCa vs. control categories of breath samples using eNose, (b) PCA analysis of PCa vs. control categories of breath samples using eNose.

On the other hand, Figure 6b represents the separation between the different prostate conditions and the healthy patients through a breath analysis, especially between the PCa patients and healthy individuals. However, some overlap is illustrated between the BPH and prostatitis groups, indicating similarities in the exhaled breath characteristics between these two conditions. In total, 79.87% of the variance is captured.

Table 4 represents the metrics showing an outstanding performance of 100% for both the PCa and control groups (BPH, prostatitis, and healthy). This indicates that the PCA-SVM model can completely distinguish between prostate cancer patients and healthy individuals from the dataset based on exhaled breath.

Table 4. Metrics for PCA-SVM model for classifying PCa vs. control categories with breath samples using eNose.

Breath-eNose-PCA-SVM		
Metrics	PCa (%)	Control (%)
Precision	100	100
Sensitivity	100	100
Specificity	100	100
Accuracy	100	100
NPV	100	100

A similar trend is observed in the distribution of the categories with the eTongue, demonstrating the eTongue’s ability to effectively classify patients according to their prostate condition, distinguishing between PCa patients and healthy individuals. Therefore, utilizing a DFA analysis (see Figure 7), the separation between the other groups is observed by classifying the categories with the breath samples, where the factors can be used to distinguish between different prostate diseases using learning methods.

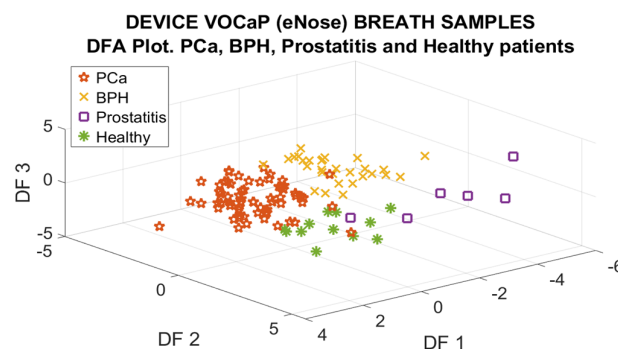


Figure 7. DFA plot of PCa vs. control categories of breath samples by using eNose.

The metrics for the DFA-KNN model indicate a high performance in classifying prostate conditions and healthy patients (see Table 5). In this case, the accuracy is high for all the groups, especially for prostatitis and healthy patients, where the classification model achieved 100% accuracy for PCa and BPH. Although the accuracy remains high, some misclassified cases indicate that some false positives occurred. Regarding sensitivity, it is notably high for PCa, BPH, and healthy patients; however, its sensitivity for prostatitis is significantly lower (66.7%), indicating that the model struggles to detect all cases of prostatitis, which could be due to the similarity of its characteristics with those of other groups. For specificity and accuracy, the percentages for the four categories exceed 90%, and the specificity shows that the model is effective at avoiding false positives, which is essential to minimize unnecessary medical interventions or overdiagnosis. The high accuracy implies that the model makes correct predictions in most cases, making it a valuable tool for classifying and diagnosing prostate conditions through evaluating exhaled breath.

Table 5. Metrics for DFA-KNN model for classifying PCa vs. BPH, prostatitis, and healthy breath samples using eNose.

Breath-eNose-PCA-SVM				
Metrics	PCa (%)	BPH (%)	Prostatitis (%)	Healthy (%)
Precision	94.2	96.5	100	100
Sensitivity	98.4	96.5	66.7	91.6
Specificity	91.4	98.8	100	100
Accuracy	95.5	95.5	95.5	95.5
NPV	97.7	98.8	98.1	99.1

3.2. eTongue Data Analysis

The following section presents the results obtained with the eTongue. Voltammetric signals were acquired, and the steady-state parameters described earlier were extracted to increase the amount of information.

3.2.1. C110 Electrode for PCa vs. Control and PCa vs. Prostatitis, HBP, and Healthy Analysis

The electrochemical responses of the urine samples from the PCa patients (orange) and the control (green) are depicted in Figure 8. The horizontal axis (x) shows the applied potential (V), while the vertical axis (y) displays the resulting current (μA) measured by the C110 electrode. The signal from the PCa patient shows a significant increase in the current, reaching up to 140 μA when the applied potential is around 1 V, indicating a strong and rapid oxidation process in the PCa samples. For the control patient, a different behavior is observed, as the current value does not exceed 40 μA in the same potential range, indicating lower electrochemical activity in the control group samples and a likely different chemical composition that does not include the same disease markers present in the PCa group. The clear difference between the signals (magnitude and curve shape) indicates that cyclic voltammetry with the C110 electrode can differentiate between samples from the PCa patients and control individuals.

In the PCA analysis, based on the measurements of the urine samples using the eTongue with carbon electrodes (C110), it can be observed in both graphs that most of the variability in the data occurs in PC1, with 99.94%, meaning that most of the information for differentiating between the urine samples from the two groups is captured on this axis.

In Figure 9a, a separation between the two groups is visible, indicating that the urine samples from the PCa patients and controls have different electrochemical compositions, as detected by the electrode. However, in Figure 9b, the discrimination is not complete, as there is some overlap in the central area of the plot, demonstrating the greater complexity of the separation of the groups, especially between PCa, BPH, and prostatitis. Although

these diseases have different pathological characteristics, they affect the prostate system and urinary tract in ways that can produce similar chemical compounds (both conditions generate biochemical products, such as amino acids, nucleic acids, and proteins, related to the inflammatory process and cell growth) in urine, which may explain the overlap in the samples. It can be seen in both graphs that most of the variability in the data occurs in PC1, with 99.94%, meaning that the majority of the information gained through urine samples for the two groups is captured on this axis.

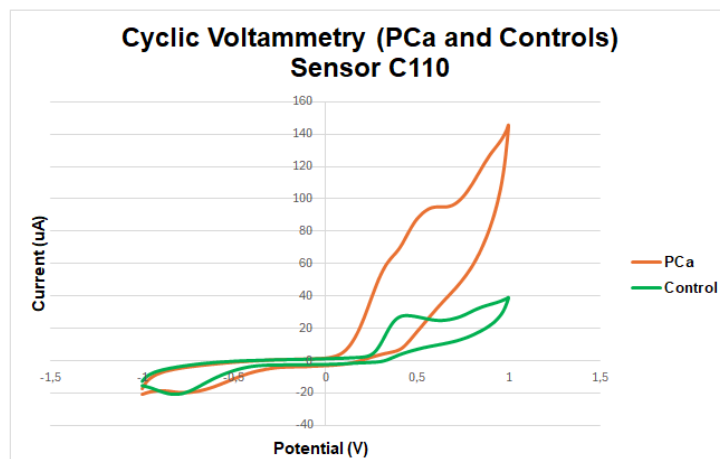


Figure 8. Signals acquired with eTongue based on C110 electrode for distinguishing between PCa (orange) and controls (green) in urine samples.

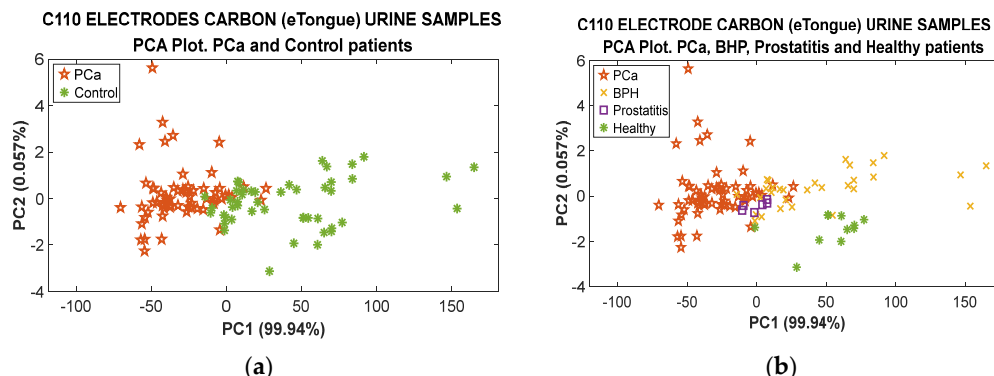


Figure 9. PCA plot of C110 electrode using eTongue. (a) PCa and control categories of urine samples and, (b) PCa vs. BPH, prostatitis, and healthy urine samples.

Table 6 presents the metrics for the results acquired using the PCA-KNN model to differentiate between the PCa patients and controls.

Table 6. Metrics for PCA-KNN model for classifying PCa vs. control urine samples using eTongue (C110 electrode).

Urine–eTongue (C110 Electrode)–PCA-KNN		
Metrics	PCa (%)	Control (%)
Precision	96.7	89.3
Sensitivity	90.0	89.3
Specificity	95.0	92.4
Accuracy	92.9	91.1
NPV	92.4	89.3

A precision of 96.7% is achieved, minimizing the number of false positives (individuals without cancer incorrectly classified as PCa, also called “False Positives”). The high sensitivity (90%), specificity (95%), and accuracy (92.9%) ensure that each category is adequately classified in each group, allowing for the successful identification of PCa patients and controls in both groups. In contrast, Figure 10 shows good separation between the samples from the PCa patients and healthy individuals, while the BPH and prostatitis categories overlap.

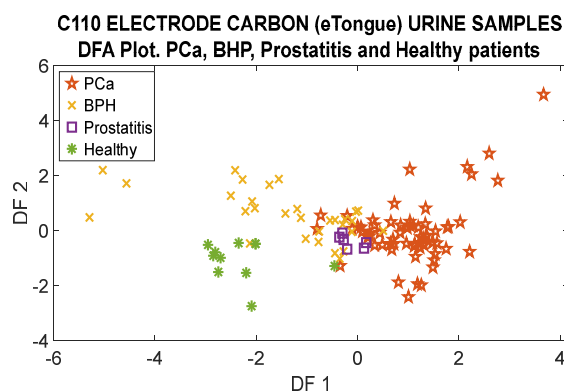


Figure 10. DFA plot of PCa and control categories for urine samples by using eTongue.

This overlap in the measurements between prostatitis and BPH is due to similar alterations in electrolyte levels, such as calcium, sodium, and potassium, which are caused by the growth of prostate tissue in BPH and inflammation in prostatitis. Since the eTongue detects variations in ionic compounds and other non-volatile metabolites, the differences in ion levels between BPH and prostatitis may not be significant enough to allow for a clear distinction between the two conditions [28,29].

Table 7 presents the metrics for the DFA-KNN model using the information extracted from the C110 electrode and the analysis of the urine samples. By comparing the results of both systems, it is observed that both technologies demonstrate 100% accuracy in detecting prostatitis, indicating an excellent performance in identifying this disease. In the case of PCa, the eTongue achieves a higher accuracy of 92.5%, compared to the eNose, which reaches 90.0%. Additionally, for patients with BPH and healthy individuals, the eNose shows better performance.

Table 7. Metrics for DFA-KNN model for classifying PCa vs. BPH, prostatitis, and healthy individuals through urine samples using eTongue (C110 electrode).

Urine–eTongue (C110 Electrode)–DFA-KNN				
Metric	PCa (%)	BPH (%)	Prostatitis (%)	Healthy (%)
Precision	92.5	89.6	100	83.3
Sensitivity	93.9	86.6	83.3	90.9
Specificity	89.3	96.3	100	98.0
Accuracy	91.1	91.1	91.1	91.1
NPV	91.3	95.2	99.0	99.0

Concerning the sensitivity, the eNose exhibited higher sensitivity at detecting PCa (95.5% vs. 93.9%) and healthy subjects (91.7% vs. 90.9%), while the eTongue was more sensitive at detecting BPH. However, the eTongue was more specific at detecting PCa (89.3%), implying a remarkable ability to avoid false positives with this diagnosis. For BPH and healthy subjects, the eNose demonstrated better specificity.

3.2.2. 250BT Electrode

Figure 11 depicts two electrical signals representing a characteristic current response as a function of the applied potential, corresponding to a voltammetric signal generated from the urine samples of patients with PCa and controls using a 250BT sensor. Observing the PCa signal, several increases in the positive and negative current peaks are generated compared to the control signal, especially in the region with a positive potential applied (from 0 to 1.5 V), which indicates more significant Redox activity in the prostate cancer samples. The difference in the current peaks may be related to specific biomarkers in the urine, whose levels or activities may change in the presence of diseases such as PCa. The above is due to particular cancer metabolites being absent in the control samples or present at lower concentrations. According to the literature, specific molecules, such as particular proteins, oxidized nucleic acids, and oxidative stress metabolites, are present at higher concentrations in cancer and can be detected electrochemically due to their ability to transfer electrons at an electrode [30,31].

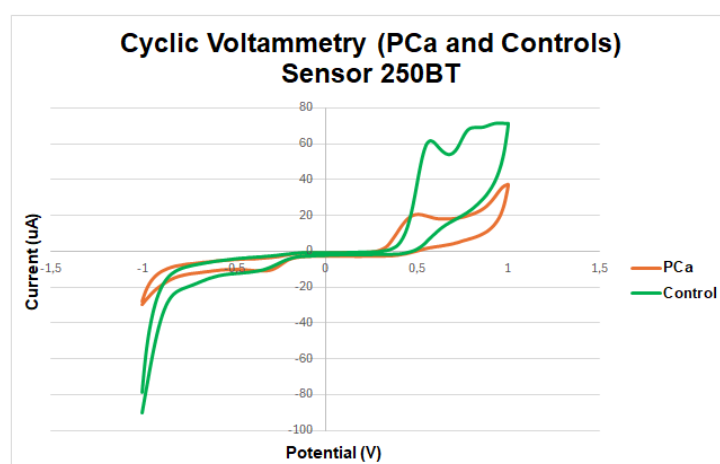


Figure 11. Signals from measurements acquired with eTongue with 250BT electrode for detecting PCa and controls using urine samples.

Figure 12a illustrates a clear separation between the PCa patients and the control group, indicating that the 250BT electrode can capture distinctive features in the urine samples that allow for differentiation between the two groups. The variance captured by PC1 explains nearly all the data variability, accounting for 99.19%. On the other hand, in Figure 12b, it can be seen that the PCa samples are mainly concentrated on the left side of the graph, near the PC1 axis, which suggests that the chemical characteristics in the PCa samples measured by the eTongue are significantly different from those of BPH, prostatitis, and healthy individuals. Additionally, the BPH samples are more dispersed and tend to cluster on the right side of the graph, away from the PCa samples; however, there is some overlap with the prostatitis and healthy samples, making the differentiation less clear when using the 250BT electrode due to the biological complexity of the compounds.

The metrics demonstrate the good performance of the PCA-SVM model at classifying the PCa vs. control urine samples with the eTongue and 250BT electrode.

Table 8 demonstrates that its accuracy and specificity for detecting prostate cancer are 100%, implying a perfect identification of the PCa patients. Although there is a slight drop in accuracy for the control group samples, the PCA-SVM model remains remarkably robust, with nearly all the performance metrics approaching 100%. This highlights the model's reliability and effectiveness at distinguishing between the PCa and control subjects with minimal error.

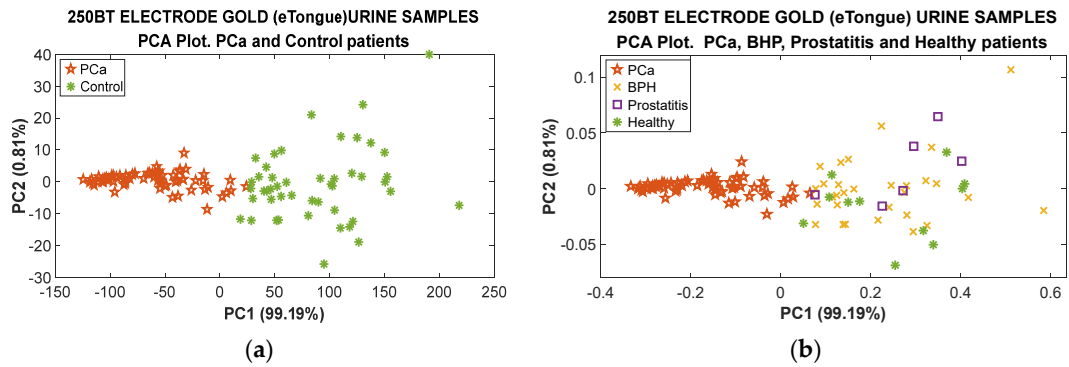


Figure 12. (a) PCA plot of PCa and control groups urine samples using 250BT electrode with eTongue. (b) PCA plot of PCa vs. BPH, prostatitis, and healthy urine samples using 250BT electrode with eTongue.

Table 8. Metrics for confusion matrix of urine samples for PCa vs. control categories classification using PCA and SVM using 250BT electrode with eTongue.

Urine–eTongue (250BT Electrode)–PCA-SVM		
Metrics	PCa (%)	Control (%)
Precision	100	97.9
Sensitivity	98.4	100
Specificity	100	98.4
Accuracy	99.1	99.1
NPV	97.9	100

In Figure 13, there is a clear discrimination between the prostate cancer and healthy patients, with minimal overlap between these two groups. However, a significant similarity is observed between the BPH, prostatitis, and healthy categories. This indicates that the eTongue system, using the 250BT electrode for urine samples, exhibits a lower performance when distinguishing between BPH, prostatitis, and healthy individuals, as the classes are not well separated. The considerable overlap between these categories indicates that the system struggles to differentiate between them, leading to reduced classification accuracy for these conditions.

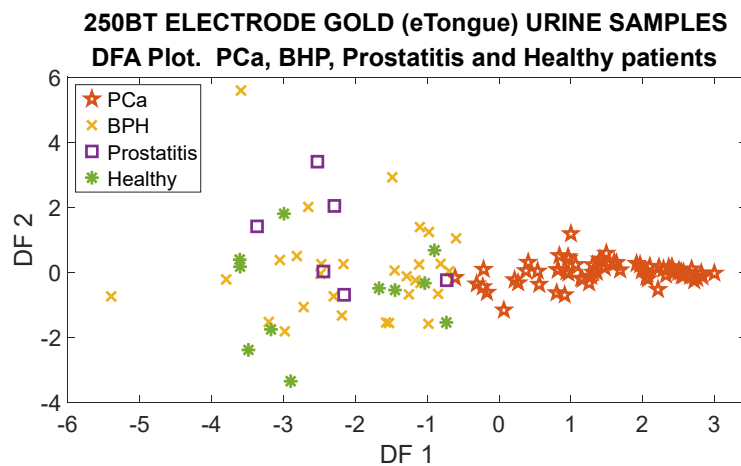


Figure 13. DFA plot of PCa and control groups urine samples acquired with –250BT electrode with eTongue.

Table 9 shows the performance of a DFA-SVM model for classifying urine samples, such as between PCa, BPH, prostatitis, and healthy individuals, using a 250BT electrode. The model demonstrates high accuracy and sensitivity at identifying PCa and BPH, but cannot correctly classify patients with prostatitis and healthy individuals, with an accuracy and sensitivity of 0% for these two categories. The overall accuracy across all the classes is 84%, and the negative predictive value is high across all the categories (around 90%), reaching 100% for BPH. In summary, this model is well suited for PCa detection, but shows limited performance for other conditions, like prostatitis, BPH, and healthy individuals, especially compared to the results reported in Table 6 for the carbon electrode, which proves more effective for classifying the control group categories.

Table 9. Metrics for confusion matrix generated through PCA and SVM model for classifying PCa vs. BPH, prostatitis, and healthy urine samples using eTongue (250BT electrode).

Urine–eTongue (250BT Electrode)–PCA-SVM				
Metrics	PCa (%)	BPH (%)	Prostatitis (%)	Healthy (%)
Precision	100	62.5	0.00	0.00
Sensitivity	98.4	100	0.00	0.00
Specificity	100	78.3	100	100
Accuracy	84.0	84.0	84.0	84.0
NPV	97.9	100	94.6	90.2

3.2.3. Combination of C110 and 250BT Electrodes

In this section, a combination of C110 and 250BT carbon/gold electrodes is applied to analyze the urine samples from patients with PCa and other related conditions. The results are processed using a PCA analysis to determine the system's ability to differentiate between these groups based on the biochemical patterns in the urine samples. Figure 14a displays the PCA results comparing the urine samples from the PCa patients and controls. The first two principal components, PC1 (88.67%) and PC2 (10.73%), account for a combined 99.40% of the total variance in the dataset, indicating that these components effectively perceive the underlying differences between the groups. Therefore, the results from Figures 8 and 11 show that it is possible to improve the discrimination between the PCa and control classes, reaching a total variance of 99.4% using PC1 and PC2.

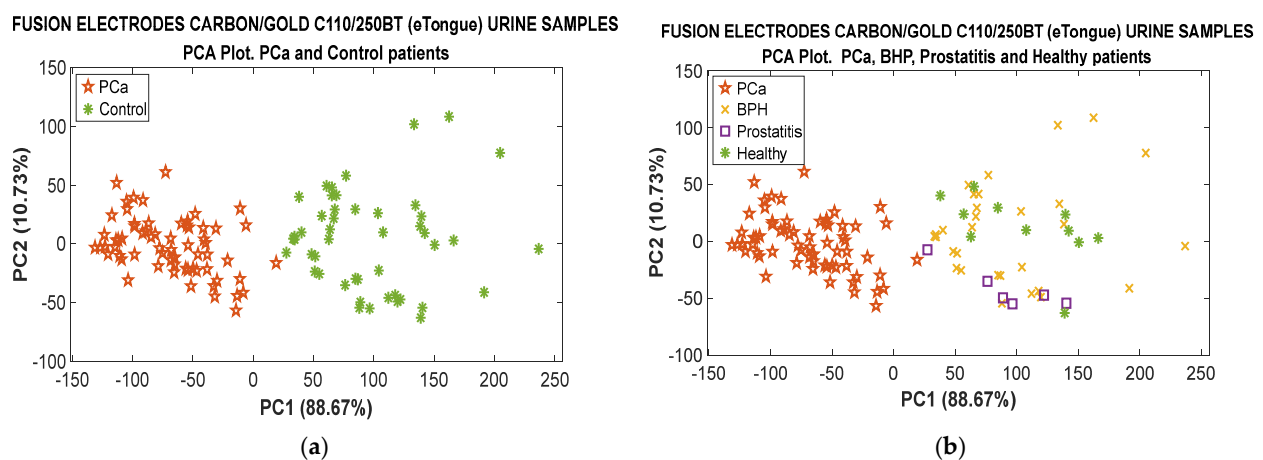


Figure 14. (a) PCA plot of PCa and control groups urine samples acquired using C110 and 250BT electrodes with eTongue. (b) PCA plot of PCa vs. BPH, prostatitis, and healthy urine samples using eTongue (C110 and 250BT electrodes).

Figure 14b illustrates the analysis of the patients with BPH, prostatitis, PCa, and healthy controls. In this case, the variance obtained by PC1 (88.67%) and PC2 (10.73%) remains the same. Though most of the control samples are not well discriminated, the trend in PCa identification shows a slight improvement.

Table 10 depicts the performance metrics of the confusion matrix for classifying the PCa and control categories derived from the PCA-SVM model with an eTongue with C110 and 250BT electrodes. These results demonstrate the system’s robustness, when equipped with both electrodes, at distinguishing between prostate cancer and the control groups using the classification model. The precision and specificity for PCa detection reaches 100%, meaning that all the positive predictions for PCa are correct.

Table 10. Metrics for confusion matrix of breath samples for PCa vs. control categories classification using PCA and SVM using C110 and 250BT electrodes with eTongue.

C110/250BT–eTongue (Urine)–PCA-SVM		
Metrics	PCa (%)	Control (%)
Precision	100	97.9
Sensitivity	98.4	100
Specificity	100	98.4
Accuracy	99.1	99.1
NPV	97.9	100

The DFA plot in Figure 15 shows the classification of the urine samples from the patients with PCa and related conditions. The analysis with C110 and 250BT electrodes demonstrates its ability to classify the samples and highlights its potential as a diagnostic tool for PCa detection. While BPH and prostatitis show some overlap, the overall classification of healthy individuals and those with prostate conditions remains robust.

FUSION ELECTRODES CARBON/GOLD C110/250BT (eTongue) URINE SAMPLES

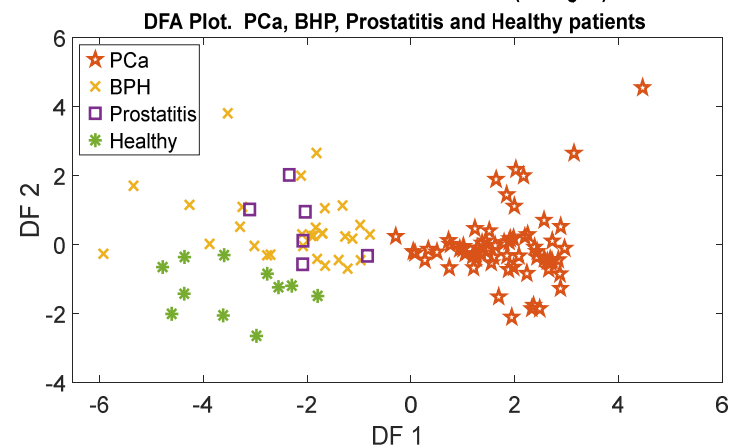


Figure 15. DFA plot of PCa vs. BPH, prostatitis, and healthy urine samples acquired with eTongue (C110 and 250BT).

Table 11 shows the performance metrics for classifying PCa and related prostate diseases based on urine samples using the DFA and SVM models with the C110 and 250BT electrode responses. The highest accuracy is observed for the DFA-SVM model using the C110/250BT electrodes, with the urine samples showing a consistent accuracy of 92% across all the categories, compared with the accuracies calculated in Tables 6 and 8.

Table 11. Metrics for DFA and SVM model for classifying PCa vs. BPH, prostatitis, and healthy urine sample measurements through eTongue (C110/250BT).

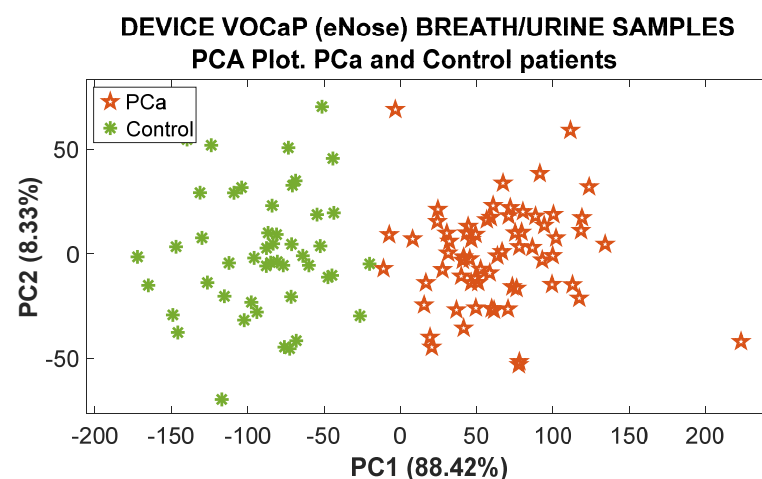
C110/250BT–eTongue (Urine)–DFA-SVM				
Metrics	PCa (%)	HPB (%)	Prostatitis (%)	Healthy (%)
Precision	100	84.3	50.0	90.0
Sensitivity	98.4	90.0	50.0	81.8
Specificity	100	93.9	97.2	99.0
Accuracy	92.0	92.0	92.0	92.0
NPV	97.9	96.3	97.2	98.0

3.3. Data Fusion of the “E-Senses” Devices

This section describes the results for the data fusion of both systems, specifically aimed at enhancing the detection of PCa. Therefore, by integrating the data from both systems, we seek to determine whether their combination can significantly improve classification accuracy, increase sensitivity, and optimize additional performance metrics.

3.3.1. Data Fusion of Breath and Urine Samples Through eNose

Figure 16 details the PCA analysis of the combination of the VOCs emitted from the breath and urine samples acquired with the eNose to increase the detection capability using the two datasets. The newly constructed dataset allows for a broader and more precise detection of the compounds associated with PCa and other disease states, improving diagnostic reliability. PC1, accounting for 88.42% of the variance, clearly discriminates between the PCa patients and controls, with the two groups mostly separated along the PC1 axis. The results indicate that the eNose system can effectively distinguish between PCa patients and healthy individuals when analyzing the VOCs from both biological samples. While there is some overlap between the two groups, the overall trend demonstrates strong discriminatory power, indicating that the combination of the breath and urine data significantly enhances the detection of prostate cancer. This highlights the potential of the eNose system for non-invasive PCa diagnosis.

**Figure 16.** PCA plot of PCa and control groups with breath and urine measurements acquired with eNose system.

The PCA loadings plot (Figure 17) reveals which gas sensors contribute most to this separation. Sensors like SGP30 [EtOH] and MiCS4514 [OX] have strong loadings on PC1, indicating they are crucial for distinguishing PCa from the controls. The sensors with significant loadings on PC2 (like MiCS6814 [NH₃] and MiCS6814 [NO₂]) capture more subtle variations among the control groups. These loadings help to identify the

15 gas sensors that discriminate between the PCa and control patients based on breath and urine measurements.

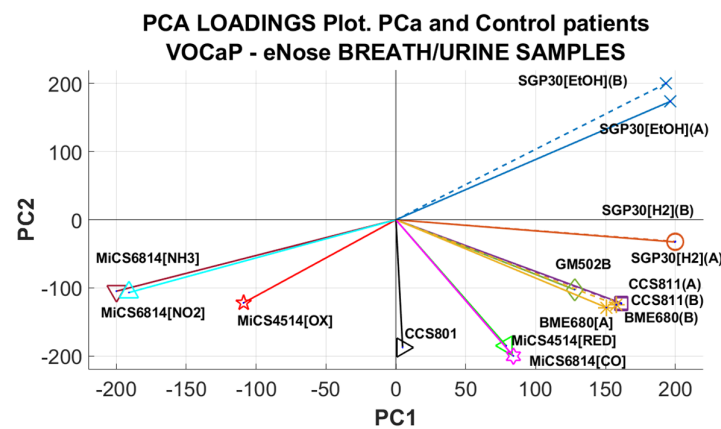


Figure 17. PCA loadings plot for PCa and control groups with breath and urine measurements acquired with eNose system.

Table 12 demonstrates a perfect classification performance when employing a PCA and decision trees model for distinguishing between the PCa and control categories through both types of samples. With all the metrics at 100%, the model shows no misclassification, signifying that the combination of PCA and decision trees with the eNose system is highly significant for accurately detecting prostate cancer based on the two biological samples. This level of performance implies excellent discriminatory power between the two groups.

Table 12. Metrics derived for PCA and decision trees classification of PCa vs. control categories based on breath and urine samples using eNose.

eNose (Breath/Urine)-PCA-Decision Trees		
Metrics	PCa (%)	Control (%)
Precision	100	100
Sensitivity	100	100
Specificity	100	100
Accuracy	100	100
NPV	100	100

The PCA plot in Figure 18 shows the discrimination of PCa and related conditions based on breath and urine measurements through the eNose system. Although the PCa and healthy individuals are well separated, there is an overlap between BPH and prostatitis, indicating that their VOCs profiles are more similar, making them difficult to differentiate. In summary, the 96.78% variance obtained demonstrates the strong performance of the eNose system, particularly for identifying PCa. However, it also indicates some difficulties distinguishing between BPH and prostatitis, hinting that the VOCs profiles of these conditions may share similarities that complicate their classification. In this case, the SGP30 [EtOH, H₂] and CCS811 gas sensors can distinguish PCa, while the MiCS6814 [NH₃, NO₂] sensor helps separate the healthy groups. Additionally, the remaining sensors, including CCS801, MiCS4514 [RED], GM502B, BME680, and CCS811, contribute to differentiating between BPH and prostatitis by influencing both PCs.

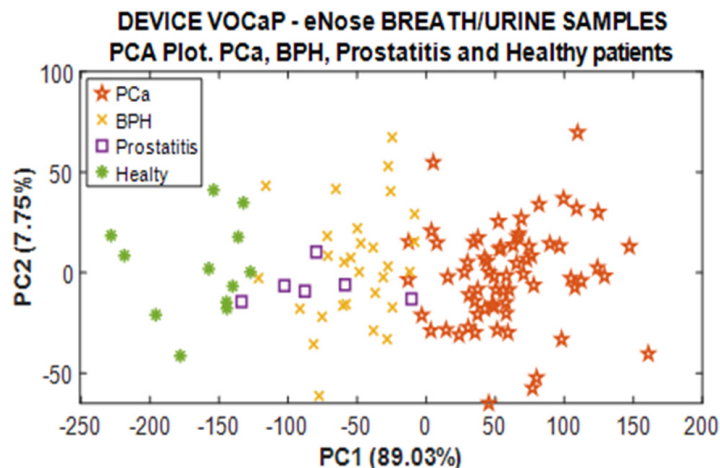


Figure 18. PCA plot of prostate cancer and related disease categories through breath and urine measurements acquired with eNose system.

Alternatively, Figure 19 illustrates a DFA plot showcasing the eNose system’s classification performance in distinguishing between those categories. As it can be seen, the system demonstrates a good separation between the PCa and healthy groups, with minimal overlap. Nevertheless, some overlap is observed between the BPH and prostatitis categories, indicating similarities in their VOCs profiles, which makes these two conditions difficult to classify. In addition, partial similarities are seen between the BPH and PCa samples, suggesting that specific BPH profiles may slightly resemble those of PCa patients, complicating the classification of these two groups. Despite this, the eNose system shows robust separation between the PCa and healthy individuals.

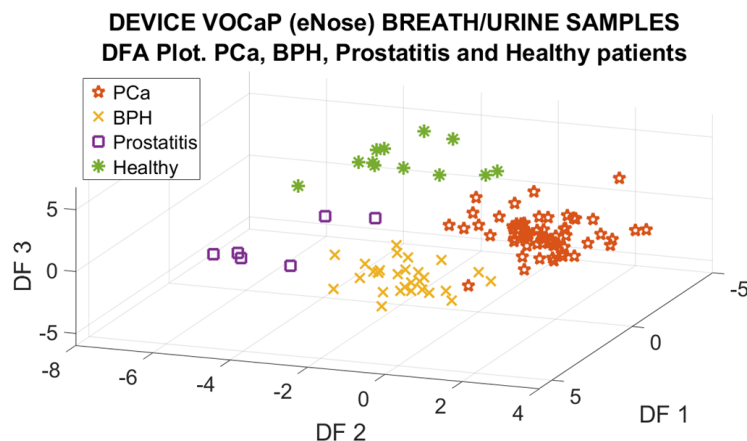


Figure 19. DFA plot of prostate cancer and related disease categories through breath and urine measurements acquired with eNose system.

The classification performance of the eNose system, employing DFA and KNN to distinguish between all the categories (PCa, BPH, prostatitis, and healthy individuals) is detailed in Table 13. The data fusion of the breath and urine samples achieves perfect scores of 100% for precision, sensitivity, specificity, accuracy, and NPV for prostatitis and healthy categories. In addition, it performs outstandingly well at PCa classification, with 100% sensitivity, 99.1% accuracy, and 98.5% precision. Its sensitivity for BPH classification is slightly lower, reaching 96.5% and an NPV of 98.8%, but still performs strongly.

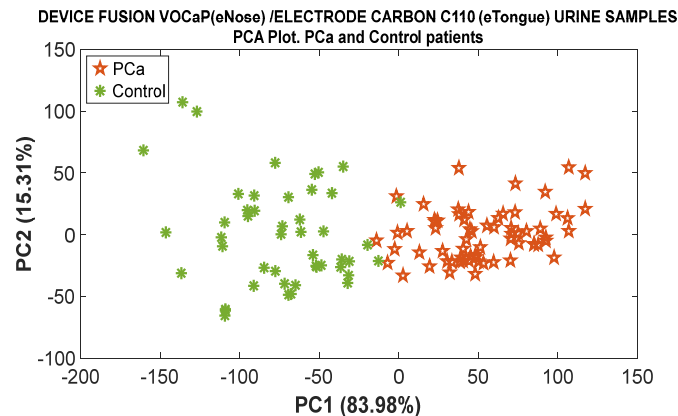
Table 13. Metrics for breath and urine samples using DFA and KNN model for classifying PCa vs. BPH, prostatitis, and healthy measurements through eNose system.

eNose (Breath/Urine)–DFA-KNN				
Metrics	PCa (%)	BPH (%)	Prostatitis (%)	Healthy (%)
Precision	98.5	100.0	100	100
Sensitivity	100	96.5	100	100
Specificity	97.8	100	100	100
Accuracy	99.1	99.1	99.1	99.1
NPV	100	98.8	100	100

The system demonstrates an outstanding classification performance, particularly for PCa, prostatitis, and healthy individuals, compared with the results for the metrics in Tables 2–8.

3.3.2. Data Fusion of eTongue and eNose Data for Urine Sample Analysis

This first combination corresponds to the data acquired through the eNose and eTongue (C110 electrode) with urine samples, where the PCA plot depicts the data fusion applied to the urine samples from the PCa and control patients. The results show that PC1 explains 83.98% of the variance, while PC2 accounts for 15.31%. As can be seen, there is a clear trend of separation between the PCa and control groups; however, some overlapping between the two clusters is evident, particularly along the PC1 axis (see Figure 20). This overlap indicates that while the both systems, in combination, are effective at distinguishing between the two categories, some similarities in the chemical profiles of the samples exist.

**Figure 20.** PCA plot of prostate cancer and control categories through urine samples acquired with eNose and eTongue (C110 electrode) systems.

It should be noted that the confusion matrices obtained from Figures 21, 23, 25, 27 and 30 were applied to determine the performance of the best classifier for detecting the PCa and control samples, which were used to calculate the metrics associated with each model.

The confusion matrix in Figure 21 represents the performance of a PCA-SVM classification model applied to the urine samples to distinguish between the PCa and control patients using a combination of the eTongue system with a carbon electrode (C110) and the eNose. The matrix shows that the model correctly classifies 65 PCa samples and misclassifies one as a control, resulting in 98.5% of the PCa samples being correctly identified. Of the control samples, 100% are correctly identified. The model is 97.9% accurate at classifying the control samples, with a 2.1% error rate for control predictions.

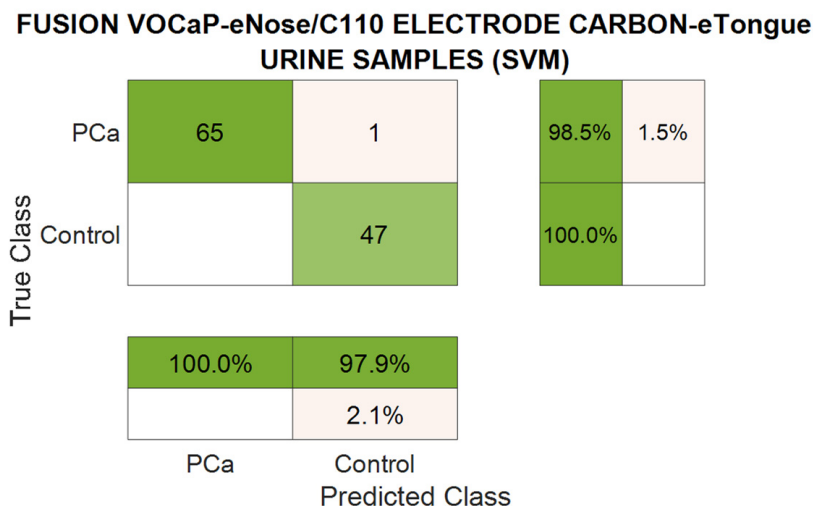


Figure 21. Confusion matrix obtained from PCA-SVM classification model for urine samples (PCa vs. control) using eNose and eTongue (C110 electrode).

Table 14 summarizes the key performance metrics obtained for the PCA-SVM classification model applied to urine samples to distinguish between the PCa and control patients using data from the eNose and eTongue (C110 electrode) systems. The model performs well, with 100% precision for PCa and 97.9% for the controls, indicating a low false-positive rate. The sensitivity reaches 98.4% for PCa and 100% for the controls, representing a near-perfect detection of PCa cases and no missed control cases. The method also achieves 100% specificity for PCa, ensuring no misclassification of healthy controls as PCa, while the specificity for the controls is slightly lower at 98.4%. The model's overall accuracy is 99.1% for both categories, reflecting its robustness. Lastly, the NPV for the model is 97.9% for PCa and 100% for the controls, highlighting the model's reliability at correctly identifying true negatives, which is crucial for minimizing missed diagnoses in clinical applications.

Table 14. Metrics derived for PCA-SVM model through urine samples of PCa vs. control categories using eNose and eTongue (C110 electrode).

eNose (Urine)–eTongue (Urine)–PCA-SVM		
Metrics	PCa (%)	Control (%)
Precision	100	97.9
Sensitivity	98.4	100
Specificity	100	98.4
Accuracy	99.1	99.1
NPV	97.9	100

Figure 22 shows that the DFA plot provides more precise visual separation between the PC and control categories compared to the PCA; it also introduces more classification errors, as demonstrated by some overlap in the DFA plot. This may be because the DFA, while optimized for class separation, can overfit the data or be less flexible in handling complex, nonlinear relationships between features. Despite showing more overlap visually, the PCA might have a more balanced approach to capturing the underlying variance in the data, which could explain the fewer misclassifications.

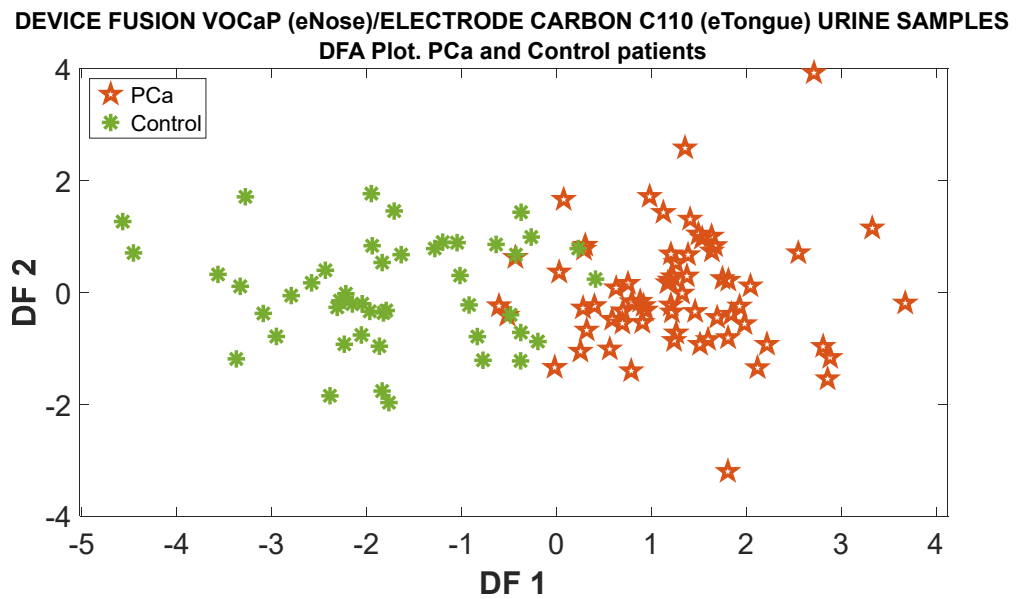


Figure 22. DFA classification of prostate cancer and control categories through breath and urine samples acquired with eNose and eTongue (C110 electrode) systems.

The confusion matrix in Figure 23 shows the classification results from a DFA-SVM model applied to urine samples for detecting PCa and control patients, combining the eNose and eTongue (C110) information.

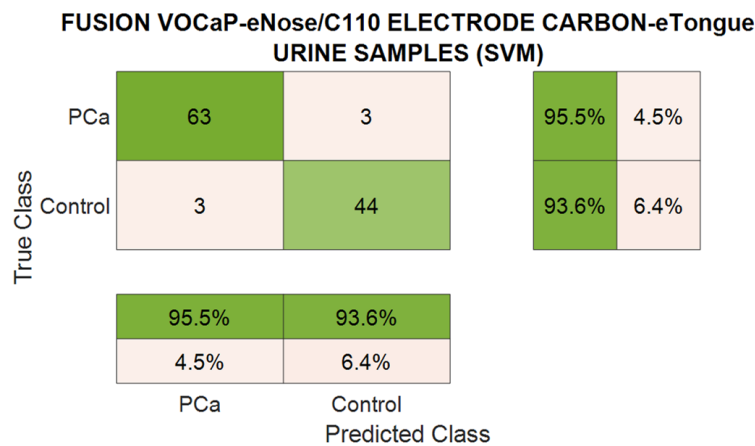


Figure 23. Confusion matrix obtained from DFA-SVM classification model of urine samples (PCa vs. control) using eNose and eTongue (C110 electrode).

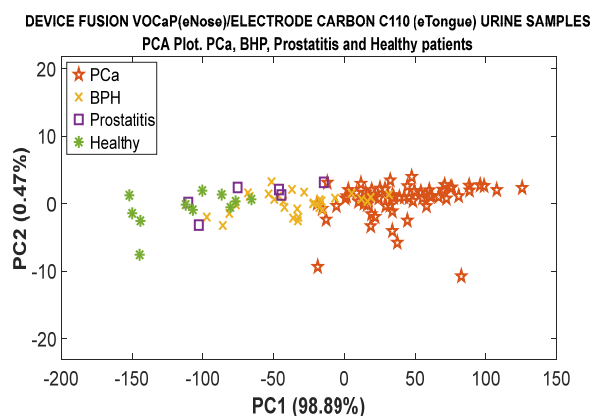
The matrix indicates high accuracy in both categories: for the PCa patients, 63 out of 66 samples are correctly classified (95.5%), with only three misclassified as controls. Similarly, 44 out of 47 control samples are correctly identified (93.6%), with three measurements misclassified as PCa. The overall performance shows a good discrimination ability between the two groups with minimal error rates, reflecting the model’s efficacy. The DFA-SVM model accurately classifies 95.5% of the PCa and 93.6% of the control samples.

Table 15 summarizes the metrics calculated for the DFA-SVM classification model. The model, applied to urine samples using both systems, shows strong performance at classifying the PCa and control patients. The precision, sensitivity, and accuracy for both categories are high, with 95.4% for PCa and slightly lower values for the control (93.6%). The DFA-SVM model’s reliability in distinguishing between the PCa and control patients is high.

Table 15. Metrics derived for DFA-SVM model using urine samples of PCa vs. control categories using eNose and eTongue (C110 electrode) systems.

eNose (Urine)–eTongue (Urine)–DFA-SVM		
Metrics	PCa (%)	Control (%)
Precision	95.4	93.6
Sensitivity	95.4	93.6
Specificity	93.6	95.4
Accuracy	94.6	94.6
NPV	93.6	95.4

The following PCA plot (see Figure 24) demonstrates the ability of the combined eNose and eTongue systems using a C110 carbon electrode to differentiate PCa from related conditions through a urine sample analysis.

**Figure 24.** PCa plot of prostate cancer and related conditions categories through urine measurements acquired with eNose and eTongue (C110 electrode) systems.

PC1 obtained 98.89% of the variance, effectively distinguishing between disease categories. The PCa patients form a distinct cluster, showing good separation from the other groups. Nevertheless, there is a notable overlap between BPH, prostatitis, and healthy patients.

Through the following confusion matrix, the model accurately detects PCa with a 95.5% accuracy, correctly classifying 63 out of 66 samples (see Figure 25). Its BPH classification has a 64.4% sensitivity, with some misclassification in the PCa group, reflecting the overlap observed in the PCA plot. Thus, prostatitis is incorrectly classified, while the healthy samples have a 66.7% misclassified sample accuracy, showing some overlap with BPH. These findings are consistent with the PCA analysis and indicate that although the model performs well in detecting PCa, there is a need for further improvement to distinguish between non-cancerous conditions, like BPH, prostatitis, and healthy patients, where overlaps still exist.

The metrics for the PCA-SVM model show a good performance at detecting PCa with 100% precision, 95.4% sensitivity, and high specificity, indicating that the model is highly effective at identifying disease cases with no false positives (see Table 16). Nevertheless, while BPH is detected with perfect sensitivity, the model's moderate precision of 64.4% results in some misclassifications. Its prostatitis detection is poor, with 0% for precision and sensitivity, highlighting its significant misclassification issues. The model has a good precision of 80%, but a low sensitivity of 33.33% for healthy patients, indicating that many are incorrectly classified. The model maintains a balanced accuracy of around 84.9% across all conditions.

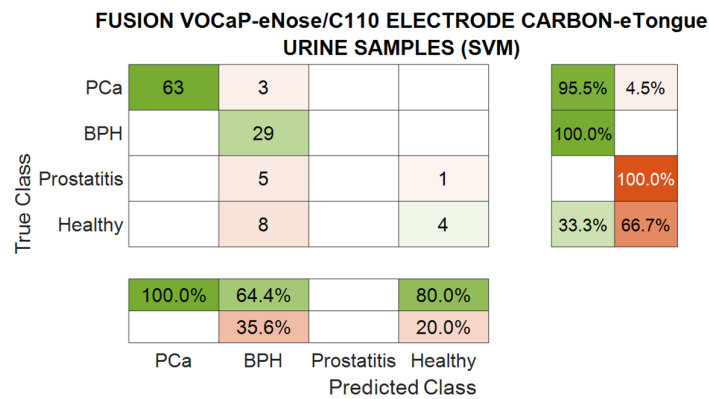


Figure 25. Confusion matrix obtained from PCA-SVM classification model of urine samples (PCa vs. related diseases) using eNose and eTongue (C110 electrode).

Table 16. Metrics derived for PCA-SVM model through urine samples of PCa vs. related disease categories using eNose and eTongue (C110 electrode).

eNose (Urine)–eTongue (Urine)–PCA-SVM				
Metrics	PCa (%)	BPH (%)	Prostatitis (%)	Healthy (%)
Precision	100	64.4	0.00	80.0
Sensitivity	95.4	100	0.00	33.33
Specificity	100	80.9	100	99.01
Accuracy	84.9	84.9	84.9	84.96
NPV	94.0	100	94.6	92.59

Figure 26 illustrates a DFA plot drawn from the urine samples measured using the eNose and eTongue systems, which are projected onto a 3D space. The PCa and BPH samples have some overlap but are primarily distinct, while the healthy samples form a separate cluster. The prostatitis samples are more spread out, indicating more significant variability and difficulty in classification. The plot demonstrates the system’s ability to distinguish between these categories, though there are overlaps, particularly between the PCa and BPH samples.

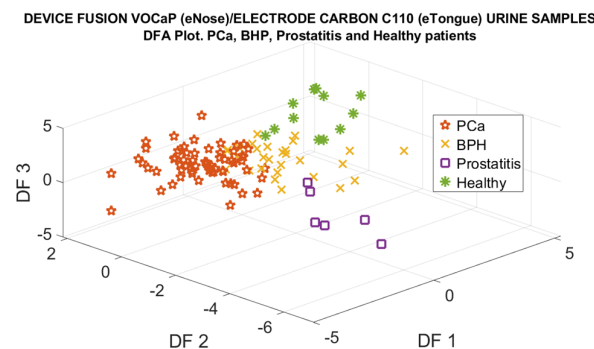


Figure 26. DFA plot of PCa and related disease categories through urine measurements acquired with eNose and eTongue (C110 electrode) systems.

The confusion matrix in Figure 27 and the metrics in Table 16 demonstrate that the DFA-SVM model performs strongly at detecting PCa and healthy individuals, achieving high precision (94–100%) and sensitivity (95.4–100%) for both classes. BPH is also well classified, with 90.3% precision and 93.3% sensitivity, although three misclassified samples overlap with PCa.

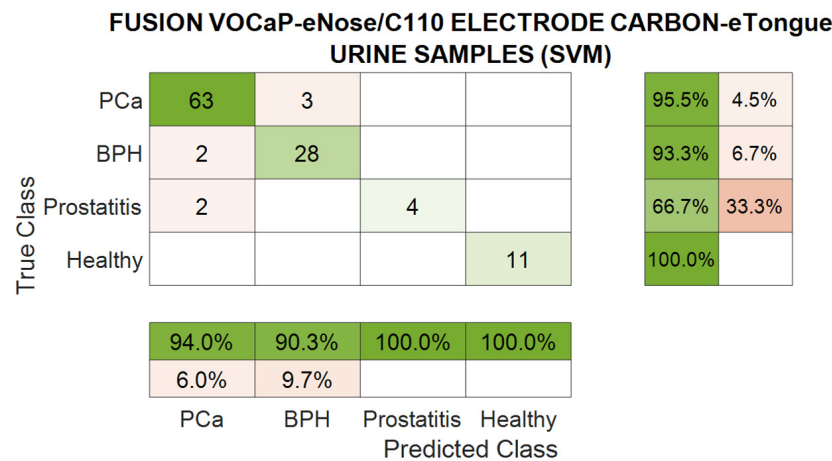


Figure 27. Confusion matrix obtained from DFA-KNN classification model of urine samples (PCa vs. related diseases) using eNose and eTongue (C110 electrode).

On the other hand, prostatitis presents more significant challenges, as the model achieves 100% precision but only 66.6% sensitivity. Although the model effectively differentiates between PCa and healthy individuals, it encounters some difficulty distinguishing BPH and prostatitis from PCa, leading to a slightly reduced accuracy in these cases (see Figure 17).

3.3.3. Data Fusion of eNose and eTongue for Analyzing Urine and Breath Samples

The PCA plot presented in Figure 28 differentiates the PCa patients from the healthy controls using breath and urine samples analyzed by the eNose and eTongue (C110/250BT electrodes) systems. In this case, the PCa patients are categorized on the left, while the healthy individuals cluster on the right, with minimal overlap. The two principal components (PC1 and PC2) reach 81.80% and 10.28% of the variance, respectively, indicating that the system effectively separates the two groups based on the sensor data.

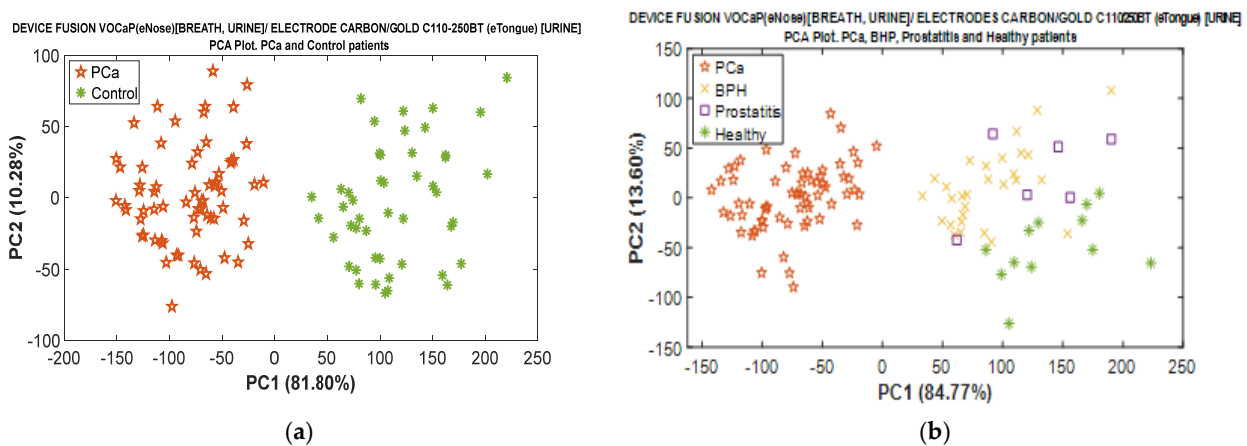


Figure 28. (a) PCA plot of prostate cancer and control categories through breath and urine measurements acquired with eNose and eTongue (C110/250BT electrodes) systems. (b) PCA plot of prostate cancer and related diseases through breath and urine measurements acquired with eNose and eTongue (C110 electrode) systems.

The metrics obtained with DFA-KNN model in Table 17 align closely with the PCA plot results, which show a clear separation between the prostate cancer (PCa) patients and control individuals, with minimal overlap.

Table 17. Metrics derived for DFA-KNN model through urine samples of PCa vs. related conditions categories using eNose and eTongue (C110/250BT electrodes).

eNose (Urine)–eTongue (Urine)–DFA-KNN				
Metrics	PCa (%)	BPH (%)	Prostatitis (%)	Healthy (%)
Precision	94.0	90.3	100	100
Sensitivity	95.4	93.3	66.6	100
Specificity	91.4	96.3	100	100
Accuracy	93.8	93.8	93.8	93.8
NPV	93.4	97.5	98.1	100

This visual distinction of Figure 28 is supported by Table 18, with 100% precision, sensitivity, specificity, and accuracy, indicating that the PCA-KNN model, when combined with data from the eNose and eTongue, effectively distinguishes between the two groups without misclassifications. Therefore, the table demonstrates that both systems, combined with the PCA and KNN models for the classification process, provide an alternative method for accurately identifying prostate cancer patients based on breath and urine samples.

Table 18. Metrics derived for PCA-KNN model through urine samples of PCa vs. related conditions categories using eNose and eTongue (C110/250BT electrodes).

eNose (Breath and Urine)–eTongue (Urine)–PCA-KNN		
Metrics	CaP (%)	Control (%)
Precision	100	100
Sensitivity	100	100
Specificity	100	100
Accuracy	100	100
Precision	100	100

Figure 29 shows the 3D DFA plot, which separates the PCa, BPH, prostatitis, and healthy individuals based on the breath and urine measurements acquired using both the eNose and eTongue systems with carbon/gold electrodes. The clear separation between the four categories indicates that the eNose and eTongue systems effectively distinguish between prostate-related conditions and healthy patients.

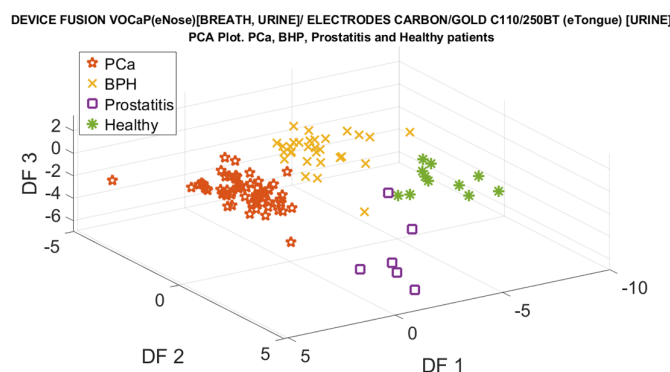


Figure 29. DFA classification of prostate cancer and related conditions through breath and urine measurements acquired with eNose and eTongue (C110/250BT electrodes) systems.

This confusion matrix demonstrates the high accuracy of the DFA-SVM model at classifying the PCa, BPH, prostatitis, and healthy individuals using breath and urine

through the combination of the eNose and eTongue (C110/250BT electrodes) information (see Figure 30).

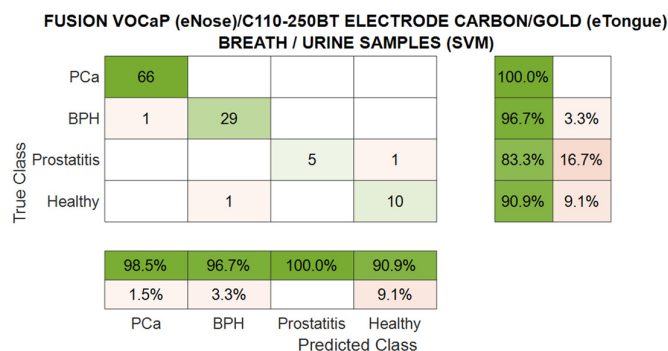


Figure 30. Confusion matrix of prostate cancer and related diseases through breath and urine measurements acquired with eNose and eTongue (C110/250BT electrodes) systems applying DFA and SVM models.

The model identifies PCa and BPH with 98.5% and 96.7% accuracy rates, respectively, and achieves 100% precision for PCa. Additionally, its performance for prostatitis is slightly lower, with 83.3% accuracy; the overall results highlight the system’s potential for the non-invasive detection of prostate-related diseases.

Table 19 illustrates the classification performance metrics obtained from the confusion matrix using the DFA-SVM model. Thus, the data acquired from the breath and urine samples using the eNose and eTongue systems with C110/250BT electrodes allows for the evaluation of four categories, where the precision shows the proportion of true positive classifications, with 100% precision for prostatitis and slightly lower values for PCa (98.5%), BPH (96.7%), and healthy individuals (90.9%). By contrast, the sensitivity reflects the model’s ability to detect true positives, achieving 100% for PCa and BPH but only 83.3% for prostatitis. Specificity, which measures the correct identification of true negatives, is high across all the categories, reaching 100% for prostatitis and at least 97.8% for the others. The accuracy for all the groups is uniformly high at 97.3%, indicating an overall excellent classification performance. The NPV indicates a good performance, with perfect scores for PCa and nearly ideal scores for prostatitis, BPH, and healthy individuals, suggesting a low rate of false negatives in these categories.

Table 19. Metrics for DFA-SVM model through urine and breath samples of PCa vs. related disease categories using eNose and eTongue (C110/250BT electrodes) systems.

eNose (Breath/Urine)–eTongue (Urine)–DFA-SVM				
Metrics	PCa (%)	BPH (%)	Prostatitis (%)	Healthy (%)
Precision	98.5	96.7	100%	90.9
Sensitivity	100	96.7	83.3%	90.9
Specificity	97.8	98.8	100%	99.0
Accuracy	97.3	97.3	97.3%	97.3
NPV	100	98.8	99.0%	99.0

4. Discussion

The analysis of the metrics obtained from the C110 and 250BT electrodes, individually and in combination, reveals significant insights into their performance. The C110 electrode demonstrated strong results across most metrics, particularly excelling at identifying patients with prostatitis and healthy individuals. While its accuracy at identifying healthy patients was slightly lower at 83.3%, its sensitivity was consistently high across

all categories. Notably, its sensitivity for PCa reached 93.9%, and for healthy patients it was 90.9%. These results highlight the carbon electrode's ability to differentiate between all four diagnostic categories effectively. In contrast, the performance of the 250BT electrode was more limited. While it achieved high accuracy and specificity for the PCa and BPH categories, it failed to accurately predict prostatitis and identify healthy patients, with both the accuracy and sensitivity dropping to 0%. This suggests that the gold electrode is less reliable for these categories.

However, the data fusion of both electrodes significantly improved the system's performance, particularly for classifying patients with prostatitis and healthy individuals. Although the results for prostatitis were moderate, the combined accuracy and sensitivity were satisfactory. Across all categories the key metrics, such as accuracy, specificity, and NPV, were high, reinforcing the idea that electrodes with different materials offer varied sensitivity and selectivity toward specific compounds or biochemical patterns. This indicates that each electrode reacts differently to various ions and chemicals and combining them in the eTongue enhances the information gained. As a result, the fusion of electrodes led to improved classification accuracy, which is crucial for diagnosing complex conditions like PCa, where minimizing false negatives (to avoid missing critical cases) and false positives (to prevent unnecessary treatments) are essential.

Alternatively, comparing the data fusion using the eTongue (Section 3.2.3), the eNose system demonstrated superior sensitivity, specificity, and accuracy results. It was more capable of correctly identifying the four categories, especially for detecting prostate cancer and related diseases. In addition, combining urine and breath samples analysis using an electronic nose could be a more effective method for PCa detection. While the electronic tongue benefits from data fusion, the electronic nose appears to outperform it in key diagnostic metrics, making it a more powerful tool for comprehensive disease detection. Similarly, the data fusion results from the analysis of the two biological samples acquired with the eNose achieved superior classification levels across the categories proposed in this study, reaching precision, sensitivity, and specificity values of 100% for the classification of the categories. These outcomes were compared with the results from the analysis of urine and breath samples when used individually in each system, as evidenced by the sensitivity and specificity values, with their precision and accuracy ranging from 94.2% to 100%, showing a better performance at classifying the breath samples than urine samples. It should be noted that these values correspond to conditions such as prostatitis and healthy individuals.

Although both analyses provided significant results when conducted separately, the data fusion technique improved the accuracy and consistency of disease identification, as each biological sample contributed a different part of the body's metabolic profile. For instance, exhaled breath VOCs are of endogenous origin, resulting from metabolic processes released and distributed into the bloodstream, entering the air in the lungs through diffusion across the pulmonary alveolar membrane, and appearing in the exhaled breath. On the other hand, urine VOCs are generated through the excretory system, offering a complementary view of the metabolic state [32,33]. Urine analysis has traditionally been used to detect urological disorders, infections, and cancer, as urine directly reflects the metabolic waste products from the blood and kidneys [34,35]. This is why, by fusing the data from biological matrices such as the breath and urine, and analyzing them with the eNose, valuable information about a patient's metabolic state can be captured, improving the robustness of the model and ultimately providing a more reliable and effective diagnostic tool for detecting complex diseases, such as prostate cancer [36]. Through this study, it is demonstrated that the combination of data from both the eTongue and eNose offers a promising alternative for detecting prostatic diseases (PCa, BPH, and prostatitis) and healthy individuals by detecting VOCs and non-volatiles (ions, metabolites, and other dissolved molecules). However, it is noteworthy that the analysis of the breath and urine samples using only the eNose yielded better results, indicating that this device performs

better when combining the two data sets, which increases the information about a patient's metabolic state and overall health.

Finally, as presented in Section 3.3.2, the eNose data (breath and urine samples) and the eTongue data (urine samples) identified high PCa values with 100% sensitivity and 97.8% specificity, corresponding to the high precision of cancer identification achieved by both devices. These high values indicate that these systems can be used as reliable tools for the early diagnosis of such diseases.

5. Conclusions

The data fusion of eNose and eTongue devices demonstrated a marked improvement in detecting and classifying prostate cancer and related conditions, such as prostatitis and BPH, including healthy cases. The combined methods achieved a higher accuracy than using each device individually, underscoring the potential of integrated sensory technologies for more precise diagnostics.

The eNose performed best at classifying the four categories of prostate-related conditions and healthy patients by analyzing the volatile organic compounds (VOCs) in the breath and urine samples. Specifically, the eNose showed outstanding accuracy and sensitivity at distinguishing between PCa and healthy individuals, with near-perfect classification metrics (up to 100% in some cases). The eNose could also clearly separate PCa patients from those with BPH and prostatitis. However, there was some overlap between BPH and prostatitis, likely due to similarities in the VOCs profiles for these conditions. The eNose also demonstrated its ability to differentiate between pathological conditions and healthy patients. It is an effective non-invasive prostate cancer diagnosis tool, particularly when paired with appropriate machine learning models, such as SVM and PCA.

The application of advanced machine learning algorithms, such as SVM, PCA, and DFA, played a crucial role in improving the classification of prostate conditions. This study highlighted how proper data preprocessing and dimensionality reduction can optimize the performance of sensory data in clinical diagnostics. These portable and cost-effective devices make them highly suitable for implementation in low-resource settings. This could enhance access to prostate cancer diagnostics in rural areas, where traditional medical infrastructure may be lacking, making early detection more accessible.

This study proved that using breath and urine samples, non-invasive diagnostic techniques, could effectively detect PCa. These methods could reduce reliance on invasive procedures like biopsies, lowering patient discomfort and the risk of unnecessary interventions caused by false positives.

Future research should involve more significant and more diverse clinical trials to strengthen the generalizability of the findings. This would ensure that the sensory devices perform consistently across different populations and further validate their clinical utility compared to standard diagnostic methods. On the other hand, GC-MS should be used to complement the eNose and eTongue systems by identifying the specific biomarkers responsible for their sensor responses. This would allow for a direct comparison between the precision of GC-MS and the practical reliability of sensory devices for identifying PCa and related conditions, providing a more comprehensive understanding of the strengths and limitations of both systems.

Compared to the studies reported on in the literature, the main advancement of this research is the combination of different data obtained from both devices when analyzing different biological matrices. Additionally, classification errors between benign conditions, such as prostatitis or benign hyperplasia, and between prostate cancer and healthy patients were minimized, achieving 100% accuracy. Using machine learning algorithms, such as SVM, KNN, and Random Forest, combined with advanced preprocessing techniques (like orthogonal signal correction), allows for superior sensitivity, specificity, and accuracy performance.

6. Patents

A patentability process is underway with the Superintendence of Industry and Commerce for the eNose technology, registered under the code NC2024/0000087.

Author Contributions: Conceptualization, C.M.D.A. and J.K.C.G.; methodology, J.K.C.G., C.M.D.A. and C.A.C.V.; validation, C.A.C.V. and J.K.C.G.; investigation, C.M.D.A., J.K.C.G., C.A.C.V. and J.B.L.; writing—original draft preparation, C.M.D.A., J.K.C.G., C.A.C.V. and J.B.L.; writing—review and editing, C.M.D.A., J.K.C.G. and J.B.L.; visualization, C.A.C.V. and C.M.D.A. All authors have read and agreed to the published version of the manuscript.

Funding: This research was funded by MINCIENCIAS, grant number 112184468047 and contract number 929-2019.

Institutional Review Board Statement: URONORTE S.A. conducted the ethical review and approval for this study involving humans.

Informed Consent Statement: Informed consent was obtained from all the subjects involved in this study.

Data Availability Statement: The dataset is available upon request by emailing the authors.

Acknowledgments: The authors acknowledge the cooperation of URONORTE—Urological Center and the CEDIMOL laboratory (University of Pamplona)—for their cooperation and support during the collection and acquisition of samples.

Conflicts of Interest: The authors declare no conflicts of interest.

References

- Giona, S. Epidemiology of Prostate Cancer. *World J. Oncol.* **2021**, *10*, 63. [CrossRef]
- Oczkowski, M.; Dziendzikowska, K.; Pasternak-Winiarska, A.; Włodarek, D.; Gromadzka-Ostrowska, J. Dietary Factors and Prostate Cancer Development, Progression, and Reduction. *Nutrients* **2021**, *13*, 496. [CrossRef] [PubMed]
- Taitt, H.E. Global Trends and Prostate Cancer: A Review of Incidence, Detection, and Mortality as Influenced by Race, Ethnicity, and Geographic Location. *Am. J. Men's Health* **2018**, *12*, 1807–1823. [CrossRef]
- Culp, M.B.; Soerjomataram, I.; Efstathiou, J.; Bray, F.; Jemal, A. Recent Global Patterns in Prostate Cancer Incidence and Mortality Rates. *Eur. Urol.* **2020**, *77*, 38–52. [CrossRef]
- Hassanipour, S.; Hafshejani, A.M.; Ghoncheh, M.; Towhidi, F.; Jamehshorani, S.; Salehiniya, H. Incidence and mortality of prostate cancer and their relationship with the Human Development Index worldwide. *Prostate Int.* **2016**, *4*, 118–124. [CrossRef]
- Zhang, W.; Cao, G.; Wu, F.; Wang, Y.; Liu, Z.; Hu, H.; Xu, K. Global Burden of Prostate Cancer and Association with Socioeconomic Status, 1990–2019: A Systematic Analysis from the Global Burden of Disease Study. *J. Epidemiol. Glob. Health* **2023**, *13*, 407–421. [CrossRef]
- Jain, M.A.; Leslie, S.W.; Sapra, A. Prostate Cancer Screening. In *StatPearls*; StatPearls Publishing: Treasure Island, FL, USA, 2023. Available online: <https://www.ncbi.nlm.nih.gov/books/NBK556081/> (accessed on 17 September 2023).
- Lumbreras, B.; Parker, L.A.; Caballero, J.P.; Gómez, L.; Puig, M.; López, M.; García, N.; Hernández, I. Variables Associated with False-Positive PSA Results: A Cohort Study with Real-World Data. *Cancers* **2023**, *15*, 261. [CrossRef]
- Zniber, M.; Vahdatiyekta, P.; Huynh, T.P. Analysis of urine using electronic tongue towards non-invasive cancer diagnosis. *Biosens. Bioelectron.* **2023**, *219*, 114810. [CrossRef]
- Baldini, C.; Billeci, L.; Sansone, F.; Conte, R.; Domenici, C.; Tonacci, A. Electronic Nose as a Novel Method for Diagnosing Cancer: A Systematic Review. *Biosensors* **2020**, *10*, 84. [CrossRef]
- Scheepers, M.H.M.C.; Al-Difaie, Z.; Brandts, L.; Peeters, A.; van Grinsven, B.; Bouvy, N.D. Diagnostic Performance of Electronic Noses in Cancer Diagnoses Using Exhaled Breath: A Systematic Review and Meta-analysis. *JAMA Netw. Open* **2022**, *5*, E2219372. [CrossRef]
- Bernabei, M.; Pennazza, G.; Santonico, M.; Corsi, C.; Roscioni, C.; Paolesse, R.; Di Natale, C.; D'Amico, A. A preliminary study on the possibility to diagnose urinary tract cancers by an electronic nose. *Sens. Actuators B Chem.* **2008**, *131*, 1–4. [CrossRef]
- D'Amico, A.; Santonico, M.; Pennazza, G.; Capuano, R.; Vespasiani, G.; Fabbro, D.; Paolesse, r.; Natale, c.; Martinelli, e.; Finazzi, E. A Novel Approach for Prostate Cancer Diagnosis using a Gas Sensor Array. *Procedia Eng.* **2012**, *47*, 1113–1116. [CrossRef]
- Roine, A.; Veskimäe, E.; Tuokko, A.; Kumpulainen, P.; Koskimäki, J.; Keinänen, T.A.; Häkkinen, M.R.; Vepsäläinen, J.; Paavonen, T.; Leikkala, J.; et al. Detection of Prostate Cancer by an Electronic Nose: A Proof of Principle Study. *J. Urol.* **2014**, *192*, 230–235. [CrossRef]
- Filianoti, A.; Costantini, M.; Arriba, A.M.; Anceschi, U.; Brassetti, A.; Ferriero, M.; Mastroianni, R.; Misuraca, L.; Tuderti, G.; Ciliberto, G.; et al. Volatilome Analysis in Prostate Cancer by Electronic Nose: A Pilot Monocentric Study. *Cancers* **2022**, *14*, 2927. [CrossRef] [PubMed]

16. Capelli, L.; Bax, C.; Grizzi, F.; Taverna, G. Optimization of training and measurement protocol for eNose analysis of urine headspace aimed at prostate cancer diagnosis. *Sci. Rep.* **2021**, *11*, 20898. [CrossRef] [PubMed]
17. Bax, C.; Capelli, L.; Grizzi, F.; Prudenza, S.; Taverna, G. A novel approach for the non-invasive diagnosis of prostate cancer based on urine odour analysis. In Proceedings of the 2022 IEEE International Symposium on Olfaction and Electronic Nose (ISOEN), Aveiro, Portugal, 29 May–1 June 2022. [CrossRef]
18. Bax, C.; Prudenza, S.; Gaspari, G.; Capelli, L.; Grizzi, F.; Taverna, G. Drift compensation on electronic nose data for non-invasive diagnosis of prostate cancer by urine analysis. *iScience* **2022**, *25*, 103622. [CrossRef]
19. Nakhleh, M.K.; Amal, H.; Jeries, R.; Broza, Y.Y.; Aboud, M.; Gharra, A.; Ivgi, H.; Khatib, S.; Badarneh, S.; Har-Shai, L.; et al. Diagnosis and Classification of 17 Diseases from 1404 Subjects via Pattern Analysis of Exhaled Molecules. *ACS Nano* **2017**, *11*, 112–125. [CrossRef]
20. Peng, G.; Hakim, M.; Broza, Y.Y.; Billan, S.; Abdah-Bortnyak, R.; Kuten, A.; Tisch, U.; Haick, H. Detection of lung, breast, colorectal, and prostate cancers from exhaled breath using a single array of nanosensors. *Br. J. Cancer* **2010**, *103*, 542–551. [CrossRef]
21. Pascual, L.; Campos, I.; Vivancos, J.L.; Quintás, G.; Loras, A.; Martínez-Bisbal, M.C.; Martínez-Mañez, R.; Boronat, F.; Ruiz-Cerdà, J.L. Detection of prostate cancer using a voltammetric electronic tongue. *Analyst* **2016**, *141*, 4562–4567. [CrossRef]
22. Solovieva, S.; Karnaukh, M.; Panchuk, V.; Andreev, E.; Kartsova, L.; Bessonova, E.; Legin, A.; Wang, P.; Wan, H.; Jahatspanian, I.; et al. Potentiometric multisensor system as a possible simple tool for non-invasive prostate cancer diagnostics through urine analysis. *Sens. Actuators B Chem.* **2019**, *289*, 42–47. [CrossRef]
23. Durán, C.M.; Carrillo, J.K.; Cuastumal, C.A.; Ramos, J. Prostate Cancer Detection in Colombian Patients through E-Senses Devices in Exhaled Breath and Urine Samples. *Chemosensors* **2024**, *12*, 11. [CrossRef]
24. Calvini, R.; Pigani, L. Toward the Development of Combined Artificial Sensing Systems for Food Quality Evaluation: A Review on the Application of Data Fusion of Electronic Noses, Electronic Tongues and Electronic Eyes. *Sensors* **2022**, *22*, 577. [CrossRef] [PubMed]
25. Zaim, O.; Diouf, A.; Bari, N.; Lagdali, N.; Benelbarhdadi, I.; Ajana, F.; Llobet, E.; Bouchikhi, B. Comparative analysis of volatile organic compounds of breath and urine for distinguishing patients with liver cirrhosis from healthy controls by using electronic nose and voltammetric electronic tongue. *Anal. Chim. Acta* **2021**, *1184*, 339028. [CrossRef] [PubMed]
26. μ Stat 8000 Multi Potentiostat/Galvanostat | Metrohm. Available online: <https://www.metrohm.com/en/products/s/tat8/stat8000.html> (accessed on 24 September 2024).
27. Lee, G.; Lee, K. Feature selection using distributions of orthogonal PLS regression vectors in spectral data. *BioData Min.* **2021**, *14*, 7. [CrossRef] [PubMed]
28. Ghoshal, A.; Garmo, H.; Hammar, N.; Jungner, I.; Malmström, H.; Walldius, G.; Van Hemelrijck, M. Can pre-diagnostic serum levels of sodium and potassium predict prostate cancer survival? *BMC Cancer* **2018**, *18*, 1169. [CrossRef]
29. McNally, C.J.; Ruddock, M.W.; Moore, T.; McKenna, D.J. Biomarkers That Differentiate Benign Prostatic Hyperplasia from Prostate Cancer: A Literature Review. *Cancer Manag. Res.* **2020**, *12*, 5225–5241. [CrossRef]
30. Hayes, J.D.; Dinkova, A.T.; Tew, K.D. Oxidative Stress in Cancer. *Cancer Cell* **2020**, *38*, 167–197. [CrossRef]
31. Oh, B.; Figtree, G.; Costa, D.; Eade, T.; Hruby, G.; Lim, S.; Elfiky, A.; Martine, N.; Rosenthal, D.; Clarke, S.; et al. Oxidative stress in prostate cancer patients: A systematic review of case control studies. *Prostate Int.* **2016**, *4*, 71–87. [CrossRef]
32. Kaloumenou, M.; Skotadis, E.; Lagopati, N.; Efstathopoulos, E.; Tsoukalas, D. Breath Analysis: A Promising Tool for Disease Diagnosis—The Role of Sensors. *Sensors* **2022**, *22*, 1238. [CrossRef]
33. Zhou, M.; Wang, Q.; Lu, X.; Zhang, P.; Yang, R.; Chen, Y.; Xia, J.; Chen, D. Exhaled breath and urinary volatile organic compounds (VOCs) for cancer diagnoses, and microbial-related VOC metabolic pathway analysis: A systematic review and meta-analysis. *Int. J. Surg.* **2024**, *110*, 1755–1769. [CrossRef]
34. Llambrich, M.; Brezmes, J.; Cumeras, R. The untargeted urine volatilome for biomedical applications: Methodology and volatilome database. *Biol. Proced. Online* **2022**, *24*, 20. [CrossRef] [PubMed]
35. Wen, Q.; Boshier, P.; Myridakis, A.; Belluomo, I.; Hanna, G.B. Urinary Volatile Organic Compound Analysis for the Diagnosis of Cancer: A Systematic Literature Review and Quality Assessment. *Metabolites* **2020**, *11*, 17. [CrossRef] [PubMed]
36. Zhao, Y.; Li, X.; Zhou, C.; Peng, H.; Zheng, Z.; Chen, J.; Ding, W. A review of cancer data fusion methods based on deep learning. *Inf. Fusion* **2024**, *108*, 102361. [CrossRef]

Disclaimer/Publisher’s Note: The statements, opinions and data contained in all publications are solely those of the individual author(s) and contributor(s) and not of MDPI and/or the editor(s). MDPI and/or the editor(s) disclaim responsibility for any injury to people or property resulting from any ideas, methods, instructions or products referred to in the content.